



# Contribution of Bicarbonate Assimilation to Carbon Pool Dynamics in the Deep Mediterranean Sea and Cultivation of Actively Nitrifying and CO<sub>2</sub>-Fixing Bathypelagic Prokaryotic Consortia

Violetta La Cono<sup>1</sup>, Gioachino Ruggeri<sup>1</sup>, Maurizio Azzaro<sup>1</sup>, Francesca Crisafi<sup>1</sup>, Franco Decembrini<sup>1</sup>, Renata Denaro<sup>1</sup>, Gina La Spada<sup>1</sup>, Giovanna Maimone<sup>1</sup>, Luis S. Monticelli<sup>1</sup>, Francesco Smedile<sup>1,2</sup>, Laura Giuliano<sup>3</sup> and Michail M. Yakimov<sup>1,4\*</sup>

<sup>1</sup> Institute for Coastal Marine Environment, National Research Council, Messina, Italy, <sup>2</sup> Department of Marine and Coastal Sciences, Rutgers University, New Brunswick, NJ, United States, <sup>3</sup> Mediterranean Science Commission (CIESM), Monaco, Monaco, <sup>4</sup> Institute of Living Systems, Immanuel Kant Baltic Federal University, Kaliningrad, Russia

## OPEN ACCESS

### Edited by:

Matthew J. Church,  
University of Montana, United States

### Reviewed by:

Ingrid Obermosterer,  
FR3724 Observatoire Océanologique  
de Banyuls sur Mer (OOB), France  
Xosé Anxelu G. Morán,  
King Abdullah University of Science  
and Technology, Saudi Arabia

### \*Correspondence:

Michail M. Yakimov  
michail.yakimov@iamc.cnr.it

### Specialty section:

This article was submitted to  
Aquatic Microbiology,  
a section of the journal  
Frontiers in Microbiology

**Received:** 16 August 2017

**Accepted:** 03 January 2018

**Published:** 19 January 2018

### Citation:

La Cono V, Ruggeri G, Azzaro M, Crisafi F, Decembrini F, Denaro R, La Spada G, Maimone G, Monticelli LS, Smedile F, Giuliano L and Yakimov MM (2018) Contribution of Bicarbonate Assimilation to Carbon Pool Dynamics in the Deep Mediterranean Sea and Cultivation of Actively Nitrifying and CO<sub>2</sub>-Fixing Bathypelagic Prokaryotic Consortia. *Front. Microbiol.* 9:3. doi: 10.3389/fmicb.2018.00003

Covering two-thirds of our planet, the global deep ocean plays a central role in supporting life on Earth. Among other processes, this biggest ecosystem buffers the rise of atmospheric CO<sub>2</sub>. Despite carbon sequestration in the deep ocean has been known for a long time, microbial activity in the meso- and bathypelagic realm via the “assimilation of bicarbonate in the dark” (ABD) has only recently been described in more details. Based on recent findings, this process seems primarily the result of chemosynthetic and anaplerotic reactions driven by different groups of deep-sea prokaryoplankton. We quantified bicarbonate assimilation in relation to total prokaryotic abundance, prokaryotic heterotrophic production and respiration in the meso- and bathypelagic Mediterranean Sea. The measured ABD values, ranging from 133 to 370 μg C m<sup>-3</sup> d<sup>-1</sup>, were among the highest ones reported worldwide for similar depths, likely due to the elevated temperature of the deep Mediterranean Sea (13–14°C also at abyssal depths). Integrated over the dark water column (≥200 m depth), bicarbonate assimilation in the deep-sea ranged from 396 to 873 mg C m<sup>-2</sup> d<sup>-1</sup>. This quantity of produced *de novo* organic carbon amounts to about 85–424% of the phytoplankton primary production and covers up to 62% of deep-sea prokaryotic total carbon demand. Hence, the ABD process in the meso- and bathypelagic Mediterranean Sea might substantially contribute to the inorganic and organic pool and significantly sustain the deep-sea microbial food web. To elucidate the ABD key-players, we established three actively nitrifying and CO<sub>2</sub>-fixing prokaryotic enrichments. Consortia were characterized by the co-occurrence of chemolithoautotrophic *Thaumarchaeota* and chemoheterotrophic proteobacteria. One of the enrichments, originated from Ionian bathypelagic waters (3,000 m depth) and supplemented with low concentrations of ammonia, was dominated by the *Thaumarchaeota* “low-ammonia-concentration” deep-sea ecotype, an enigmatic and ecologically important group of organisms, uncultured until this study.

**Keywords:** dark bicarbonate assimilation, anaplerotic reactions, deep-sea microbial community, mediterranean sea, ammonium-oxidizing *Thaumarchaeota*

## INTRODUCTION

Deep aphotic pelagic water masses represent the largest marine area comprising almost three quarters of the global oceanic volume and contain majority of the global dissolved inorganic carbon (DIC) pool (Aristegui et al., 2009; Reinthaler et al., 2010). Despite that, deep-sea environment belongs by far to the least studied ecosystems on Earth. The current database contains very few data about microbial life and steering biogeochemical processes in this oceanic interim. Dark ocean carbon budgets and, especially, prokaryotic carbon demand based on carbon flux and metabolic activity are fraught with uncertainties and discrepancies (Aristegui et al., 2009; Baltar et al., 2009; Burd et al., 2010). Until recently, the deep ocean was supposed to be exclusively heterotrophic and dependent on vertical flux and lateral advection of organic carbon either produced by phytoplankton in the sunlit surface waters or entered from the atmosphere (Duarte et al., 2013). However, recent compiled global carbon budgets and intensive local field data suggest that the estimate of metabolic activity in the dark pelagic ocean exceeds estimated inputs of organic carbon (Burd et al., 2010). In some bathypelagic waters, this imbalance between carbon supply and prokaryotic carbon demand (the sum of heterotrophic biomass production and respiration) can reach about two orders of magnitude. The apparent paradox of carbon balance in dark oceans might result from the overestimation of *in situ* metabolic activities, the underestimation of organic carbon inputs from the upper layers (i.e., slowly sinking or buoyant detrital POC escaping measurements) or the existence of yet unaccounted deep-sea (autotrophic) organic carbon supply. The latter hypothesis seems more and more plausible since it goes along with recent findings on the existence of microbial bicarbonate fixation in the dark (Reinthaler et al., 2006; Steinberg et al., 2008; Tamburini et al., 2009, 2013). The existence of a positive net community production (based on local autotrophic activities) in the deep sea, would also explain the isotopic composition of the oceanic DIC, strongly depleted in  $^{13}\text{C}$  relative to atmospheric  $\text{CO}_2$  (Williams et al., 2013).

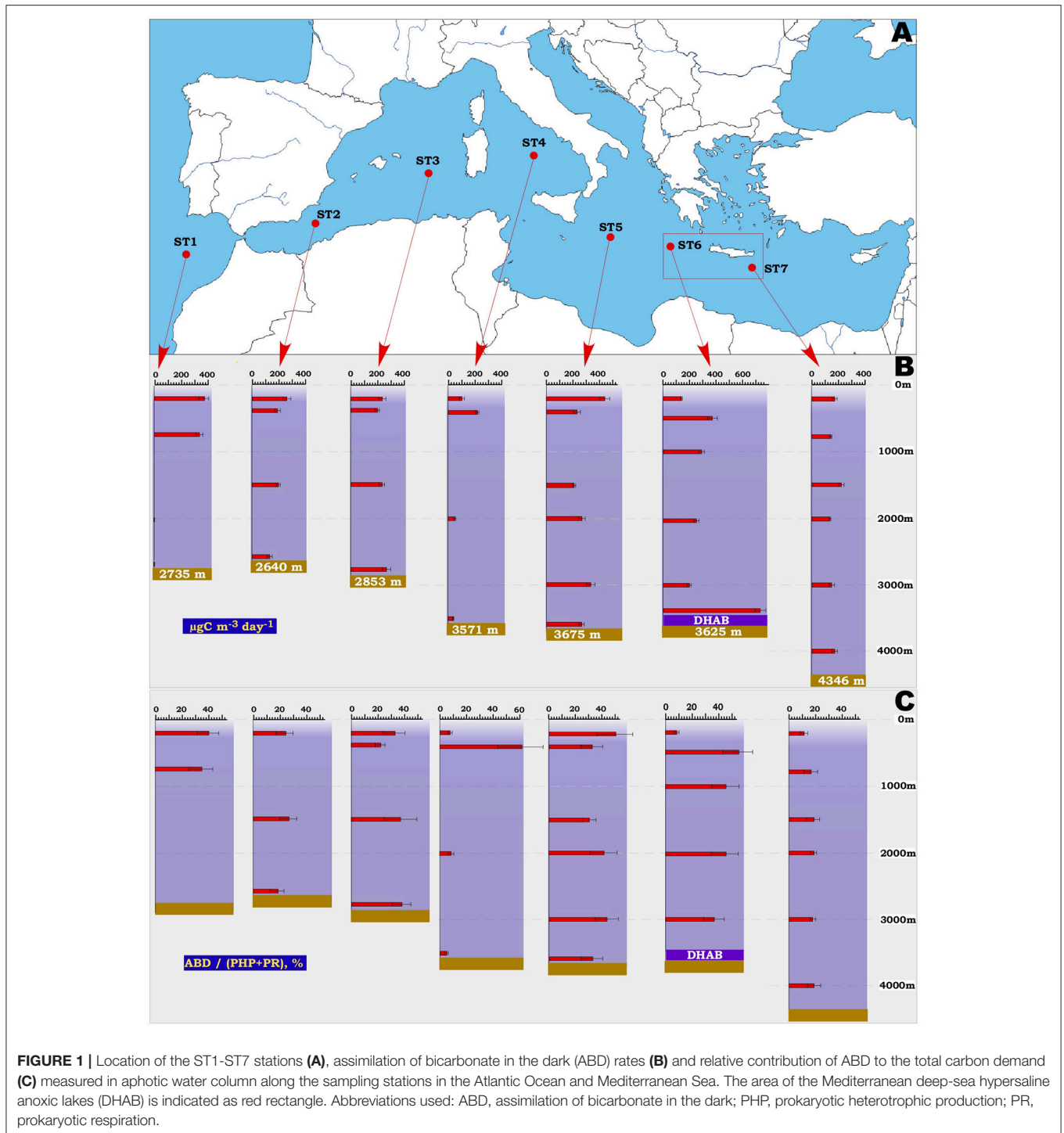
Despite its recognized importance, ABD is a still poorly understood process, which is being gathering great research attention. As to the “dark ocean,” the planktonic *Thaumarchaeota* belonging to Marine Group 1 (MG1), recently defined as the candidate order *Nitrosopumilales* (Stieglmeier et al., 2014). These tiny microorganisms (usually less than  $0.5\ \mu\text{m}$  in size) dominate the prokaryotic cell numbers in meso- and bathypelagic realms (Karner et al., 2001; Schleper et al., 2005; Ingalls et al., 2006; Varela et al., 2008) and likely play a crucial role as nitrifying autotrophs (Herndl et al., 2005; Yakimov et al., 2007, 2011; La Cono et al., 2013, 2015; Molari et al., 2013). Globally, marine ammonium-oxidizing chemoautotrophs may fix  $\sim 0.04\text{--}0.11\ \text{Pg}$  ( $\times 10^{15}\ \text{g}$ ) of inorganic carbon annually so that making a consistent input of new organic carbon to the ocean (Herndl et al., 2005; Wuchter et al., 2006; Hügler and Sievert, 2010). Thinking in numbers, dark primary production, or ABD, represents 15–53% of the photic zone’s exported production in the North Atlantic area (Reinthaler et al., 2010). Unluckily, none

MG1 representatives from the meso- and bathypelagic realms of the ocean have been yet cultivated. First cultivated representative of MG1, “*Ca. Nitrosopumilus maritimus*” SCM1, has been isolated from a seawater aquarium biofilter (Könneke et al., 2005) and other closely related cultivated organisms have recently been obtained from estuarine and arctic marine sediments (Mosier et al., 2012; Park et al., 2014) and from surface coastal waters (Qin et al., 2014; Bayer et al., 2016).

In the present study we report on microbial  $\text{DI}^{14}\text{C}$  fixation rates, respiration and heterotrophic production in the oxygenated meso- and bathypelagic waters ( $\geq 200\ \text{m}$  depth) of the Mediterranean Sea. Contrary to the Mediterranean photic layers, which are characterized by an eastward steeply decreasing gradient of trophic conditions (Siokou-Frangou et al., 2010), the Mediterranean deep-sea compartments show relatively homogeneous trends of prokaryotic heterotrophic production, bulk respiration and enzymatic activities (La Ferla et al., 2010; Azzaro et al., 2012; Luna et al., 2012; Caruso et al., 2013; Celussi et al., 2017). Our work demonstrates that ABD substantially contributes to the organic carbon demand of the Mediterranean deep-sea microbial food-web so that possibly influencing meso- and bathypelagic trophic trends in the region. By the way of an empirically optimized culturing methodology, for the first time to date, we obtained highly enriched populations of thaumarchaeal deep-sea ecotype, of which activity measurements justify the importance of ABD reactions in *de novo* formation of dark-ocean organic carbon. Thus, the present data confirm previous hypotheses on the role of DIC fixation rates in the deep Mediterranean Sea (Yakimov et al., 2007, 2011, 2014; Tamburini et al., 2009; Smedile et al., 2013; Celussi et al., 2017).

## MATERIALS AND METHODS

Seven hydrological stations, located from the Atlantic Ocean to the Levantine Sea (Eastern Mediterranean) were chosen as representatives of the main Mediterranean regions (Figure 1). Principal sampling of the west transects of Mediterranean basin (stations ST1-ST4) was conducted during a synoptic oceanographic cruise TRANSMED (May–June 2007) on board of Italian research vessels *Urania* and *Universitatis* in the framework of the VECTOR Line 8 research project. Three additional consecutive oceanographic cruises, MAMBA2010 (June 2010), MICRODEEP2012 (September–October 2012) and SALINE2014 (October–November 2014), were conducted to sample remaining three stations ST5-ST7 (Eastern Mediterranean) and six deep-sea hypersaline anoxic lakes (DHAL), all located in the Ionian Sea (Table 1). To measure conductivity, temperature, pressure and oxygen, a calibrated Seabird SBE9/11+ CTD was mounted on a General Oceanic’s rosette sampler together with 24 Niskin bottles each of 10 L volume. Seawater samples were taken from the top of aphotic water column (200 m depth) down to the seabed (30 m above the bottom). Depths, corresponding to oxygen-minimum zone and well-defined water masses, were also sampled. All 10-L Niskin bottles were equipped with silicone rubber closure and tubing that had been carefully cleaned to avoid introducing contaminants during sampling. Besides the



CTD measurements, the Winkler method (Carpenter, 1965) with an automatic burette 716 DNS Titrino (Metrohm AG, Herisau, Switzerland) was additionally carried out to measure oxygen concentration at some depths. Samples for phosphate and nitrate (20 mL) detection were directly collected from the Niskin bottles and stored at  $-20^{\circ}\text{C}$  in acid-washed polyethylene vials. Nutrient concentrations were determined in triplicates within

1 month in the laboratory, using a “SEAL QuAAtro39” high performance microflow analyzer following classical methods (Grasshoff et al., 1999). Ultra cleaned glass bottles were used for ammonium measurements to avoid contamination and  $\text{NH}_4^+$  concentration was determined fluorometrically as described elsewhere (Holmes et al., 1999; Pujó-Pay et al., 2011).

**TABLE 1** | The list of the cruises and sampling sites studied.

| Cruise        | Date       | Coordinates                   | Site name                          |
|---------------|------------|-------------------------------|------------------------------------|
| TRANSMED      | 30/05/2007 | 34° 59' 59"N,<br>08° 19' 58"W | ST1 <sup>a</sup>                   |
|               | 01/06/2007 | 36° 30' 58"N,<br>01° 00' 02"W | ST2 <sup>a</sup>                   |
|               | 03/06/2007 | 39° 19' 18"N,<br>06° 04' 47"E | ST3 <sup>a</sup>                   |
|               | 08/06/2007 | 39° 29' 57"N,<br>12° 59' 57"E | ST4 <sup>a</sup>                   |
| MAMBA2010     | 16/06/2010 | 33° 59' 42"N,<br>26° 02' 18"E | ST7 <sup>a</sup>                   |
| MICRODEEP2012 | 19/09/2012 | 35° 13' 51"N,<br>21° 28' 26"E | SAL5 <sup>a,b,c</sup>              |
|               | 20/09/2012 | 34° 40' 09"N,<br>22° 08' 42"E | DHAL <i>Thetis</i> <sup>b</sup>    |
|               | 23/09/2012 | 34° 19' 35"N,<br>22° 33' 38"E | DHAL <i>Medee</i> <sup>b</sup>     |
|               | 25/09/2012 | 34° 57' 10"N,<br>22° 01' 42"E | KRY <sup>b,c</sup>                 |
|               | 27/09/2012 | 35° 18' 19"N,<br>21° 23' 21"E | ST6 (ATA) <sup>a,b,c</sup>         |
| SALINE2014    | 28/09/2012 | 36° 29' 34"N,<br>15° 39' 34"E | ST5 <sup>a</sup>                   |
|               | 27/10/2014 | 35° 16' 37"N,<br>21° 41' 22"E | DHAL <i>Discovery</i> <sup>b</sup> |

<sup>a</sup>Study performed on aphotic water column.

<sup>b</sup>Study performed on oxic/anoxic interface of the deep-sea hypersaline anoxic lakes (DHAL).

<sup>c</sup>Site, used for enrichment setting (see Materials and Methods).

## Total Prokaryotic Abundance (PA), Heterotrophic Carbon Production (HCP), Prokaryotic Respiration (PR) and Assimilation of [<sup>14</sup>C]-Bicarbonate at the Dark (ABD)

Samples for PA, PHP, PR, and ABD were collected using 10 L Niskin bottles. Processing of the samples, lasting from water collection to incubation with the radiolabeled tracers always took less than 20 min. Epifluorescence microscopy was used for total PA determination in formalin fixed samples (2% final concentration) stained with 2,3-diamidino phenylindole (DAPI). AXIOPLAN2 Imaging microscope (Zeiss) equipped with digital camera. To obtain adequate estimates, at least 200 cells per each sample were counted and the AXIOVISION 3.1 software was used.

The PHP rates was estimated with the [<sup>3</sup>H]-leucine incorporation approach (Kirchman et al., 1985) using the micro-method developed by Smith and Azam (1992). Following this protocol, from each experimental sampling, five 2.0 mL vials (triplicate and two killed controls) were filled with 1.7 mL of seawater (maximal volume allowed). A total of 100  $\mu$ L of cold 50% trichloroacetic acid (TCA) was used to kill controls. After 15 min, 20 nmol L<sup>-1</sup> of L-[4,5-<sup>3</sup>H] leucine (144.2 Ci mmol<sup>-1</sup>; Amersham Biosciences UK Limited) was added to all samples, which were incubated in the tank for 2.5 h in the dark at *in situ*

temperature. Duplicate blanks were incubated similarly to the samples, which were after incubation killed by adding cold TCA (5% final concentration). This exposure was chosen after time course experiments, performed by PHP micro-method with meso- and bathypelagic waters during two oceanographic cruises (2006–2007) in the Central-Eastern sector of Mediterranean Sea. Rates of [<sup>3</sup>H]-leucine incorporation increased linearly over time up to 5 h and PHP values of  $\geq 94\%$  of  $V_{\max}$  has been observed for incubation between 120 and 150 min (Table S1). Obtained results were in consistence with the time course experiments, performed by Luna et al. (2012) with epi-, meso- and bathypelagic waters, collected at different stations across Mediterranean Sea (from 06°22'W to 26°41'E). The experimental determination of the isotopic dilution of leucine (ID) was done according to the kinetic method of Pollard and Moriarty (1984) using for each sample a 3 replicates and 2 TCA-killed controls, inoculated with a fixed concentration of <sup>3</sup>H-leucine (5 nmol L<sup>-1</sup>) and variable concentrations of <sup>1</sup>H-leucine (0, 2.5, 5, 10, 20, 40 nmol L<sup>-1</sup>). Our data demonstrated that 20 nmol L<sup>-1</sup> of [<sup>3</sup>H]-leucine saturated the prokaryotic incorporation and that in meso- and bathypelagic waters the isotopic dilution values varied between 1.0 and 1.33 with a mean ID = 1.28, which provides a conversion factor of 1.92 Kg C mol<sup>-1</sup> leu. The detected ID values are in accordance with those found by Van Wambeke et al. (2000) in the NE Mediterranean Sea and were used through our study in spite of the theoretical conversion factors with or without ID, previously applied for meso- and bathypelagic waters of the Mediterranean Sea (Luna et al., 2012; Celussi et al., 2017). After extraction of <sup>3</sup>H-labeled proteins (Smith and Azam, 1992), activity in the samples was determined in a Wallac 1414 liquid scintillation counter (PerkinElmer, Monza, Italy). The instrument was calibrated with internal and external standards. The blank-corrected leucine incorporation rates were converted into PHP values using the experimentally estimated ID values.

The Electron Transport System (ETS) assay based on the technique of the tetrazolium reduction (Packard et al., 1988) was used to estimate potential respiratory activity rates of the entire microbial community. Some minor modifications of the method were made to increase its sensitivity (La Ferla et al., 2003, 2005; Azzaro et al., 2006). Briefly, to remove large particles, subsamples for the analysis (10–20 L) were pre-filtered on a 200  $\mu$ m pore size mesh net and then filtered through a Whatman GF/F glass fiber membranes (0.5  $\mu$ m pore size; 47 mm diameter) at reduced pressure ( $\leq 0.3$  bar). Filters were placed into 15 mL Falcon tubes and immediately stored in liquid nitrogen until analysis in the laboratory ( $\leq 45$  days). The ETS data were corrected for *in situ* temperature with the Arrhenius equation using a value for the activation energy of 15.8 kcal/mol (Packard and Williams, 1981; Packard et al., 1988; Reinthaler et al., 2006). Obtained ETS assay values were further converted into PR rates applying the Takahashi oxygen to carbon molar ratio (Takahashi et al., 1985) and conversion PR: ETS factor of 0.68 (measurements made in mesopelagic layers of the subtropical Atlantic; Arístegui et al., 2005). Compared to other conversion factors, estimated either in nutrient-rich batch culture (Christensen et al., 1980) or in cold meso- and bathypelagic layers of North Atlantic (Reinthaler et al.,



2006), the above PR/ETS ratio produced values of the prokaryotic growth efficiency ( $PGE = PHP/[PHP+PR]$ ) in a range of 0.3–16%, coinciding with PGE values obtained by performing *in situ* marine studies (Del Giorgio and Cole, 1998 and references therein; Reinthaler et al., 2006, 2010; Azzaro et al., 2012; Celussi et al., 2017).

For ABD incubations, 40 mL of alive samples and formaldehyde-fixed blank controls were placed in 60 mL gas-tight serum bottles. The ABD rates were estimated by addition of 10  $\mu\text{Ci}$  of [ $^{14}\text{C}$ ]-bicarbonate (56.0 mCi  $\text{mmol}^{-1}$ , Amersham Italia, Milan, Italy) using a gas-tight Hamilton syringe to yield a final activity of 0.25  $\mu\text{Ci mL}^{-1}$ . Triplicate samples and duplicate formaldehyde-killed blanks were incubated in the dark at 14°C for 72 h and then stopped by the addition of formaldehyde (2% final concentration). Previously, we confirmed the linearity of [ $^{14}\text{C}$ ]-bicarbonate incorporation in microbial biomass ( $y = 0.42857 + 4.3393x$  [ $R = 0.99354$ ]) during at least 72 h of incubation time without significant changes in cell concentrations (Yakimov et al., 2014). All samples were thereafter filtered through 0.1  $\mu\text{m}$  polycarbonate filters (Millipore) and rinsed three times with 10 mL of ultra-filtered seawater. Subsequently, before addition of scintillation cocktail for [ $^{14}\text{C}$ ]-counting, the washed filters were acidified for 12 h in an HCl fume hood to remove inorganic carbon and air-dried. Filters were then stored at  $-20^\circ\text{C}$  until the radioactivity was counted in a Wallac 1414 analyser (Perkin Elmer, Monza, Italy). According to protocols of dark DIC fixation measurements (Herndl et al., 2005; Reinthaler et al., 2010), the disintegration per minute (DPM) values was calculated by subtracting the values detected in the abiotic controls from the absolute DPM obtained in the samples. Integrated ABD values ( $\text{mg C m}^{-2} \text{day}^{-1}$ ) were calculated by means of the trapezoidal method (Moutin and Raimbault, 2002) using the discrete data and assuming that rates at the bottom were identical to those of the deepest sampled depth.

The Kolmogorov-Smirnov test was used for assessing normality of datasets. To determine the significance of measured rates, One-Way or were specified Two-Ways ANOVA analysis of variance was applied. Relative importance of each treatment group was investigated by pairwise Multiple Comparisons procedures (Holm-Sidak method) with overall significance level 0.05. As described elsewhere (La Cono et al., 2013), calculations were carried out using SigmaStat software for Windows, ver. 3.1 (Copyright 1992–1995; Jandel Corporation) and differences were considered significant at  $P < 0.05$ .

## Establishment of Enrichment Cultures

Seawater samples (~1 L of volume) were collected during MICRODEEP2012 cruise from the upper interface of the brine lakes *L'Atalante* (3,499 m depth) and *Kryos* (3,338 m depth) referred to as the ATA and KRY samples, respectively. Additionally, one bathypelagic sample (3,000 m depth) was collected during the same cruise over the brine lake *Urania* (35°13'51"N; 21°28'24"E; 3,552 m depth) and referred to as the SAL5 sample (Table 1). At time of sampling, ammonium concentrations varied between 0.48  $\mu\text{M}$  (SAL5) and 120–450  $\mu\text{M}$  (ATA and KRY). Enrichment cultures were initiated by filtering

of 900 mL seawater through 0.45  $\mu\text{m}$  polycarbonate filters (Millipore) and addition of 100 mL autoclaved bathypelagic seawater supplemented with  $\text{KH}_2\text{PO}_4$  (1 mM),  $\text{NaHCO}_3$  (10 mM), Fe-NaEDTA (20  $\mu\text{M}$ ), non-chelated trace elements (10 $\times$ ), selenite-tungstate (10 $\times$ ) and vitamins (10 $\times$ ) solutions (Widdel and Bak, 1992). The pH of the medium was stabilized at 7.8 by adding of HEPES buffer (1 M HEPES, 0.6 M NaOH). In concordance with elevated ambient concentrations of ammonia in the DHAL interfaces, 500  $\mu\text{M}$   $\text{NH}_4\text{Cl}$  was added to ATA and KRY cultures. In contrast, the ammonia-impooverished bathypelagic sample SAL5 was initially supplemented with 100  $\mu\text{M}$   $\text{NH}_4\text{Cl}$ . Finally, all enrichments were supplemented with 100  $\mu\text{M}$   $\alpha$ -ketoglutarate to support eventual mixotrophic requirements of isolates (Qin et al., 2014). Cultures were incubated in the dark at 16°C without shaking. Applying the absorbance spectroscopy method (Strickland and Parsons, 1972), ammonia-oxidizing activity in the enrichment cultures was monitored by nitrite production. Additionally, microbial growth was monitored by DAPI (Glöckner et al., 1999). After reaching a plateau in nitrification, 10% (vol/vol) of the total culture volume was transferred to a fresh medium and cultivated under the same conditions. Unless otherwise stated, the enrichment cultures ATA and KRY were supplemented with 500  $\mu\text{M}$  ammonia and SAL5 with 100  $\mu\text{M}$  ammonia as energy source. The pH of the medium remained almost constant (7.6–7.8) during the culture cycle. No antibiotics were added to avoid loss of eventually antibiotic-sensitive deep-sea ecotypes.

## Gene Cloning, Sequencing, and Phylogenetic Analyses

Prokaryotic 16S rRNA and thaumarchaeal key genes involved in ammonia respiration (ammonia monooxygenase, *amoA*) and autotrophy (4-hydroxybutyryl-CoA dehydratase, *hbd*), were amplified by PCR using the primers listed in La Cono et al. (2010, 2013). All reactions were carried out in a MasterCycler 5331 Gradient PCR (Eppendorf, Hamburg, Germany) under the conditions for PCR as described elsewhere (La Cono et al., 2010, 2013; Yakimov et al., 2013). The PCR products were further purified PCR purification QIAQuick column (Qiagen, Germany) and cloned into pGEM T-Easy Vector II. After PCR verification, positive clones from each library were sequenced at Macrogen (Amsterdam, Netherlands). Pintail software (Ashelford et al., 2006) and CHECK\_CHIMERA (available from Ribosomal Database Project) were used to check sequences for possible chimeric origin. After manual checking, phylogenetic trees of the 16S rRNA gene amplified sequences and close relatives identified with BLAST (Altschul et al., 1997) were created using the ARB and SILVA alignment tools (Ludwig et al., 2004; Pruesse et al., 2007). MEGA 5 (Tamura et al., 2011) and MacVector 11.1.2 were used to align sequences of *amoA* and *hbd* functional genes. After alignment, the neighbor-joining algorithm of ARB and MEGA 5 program packages were used to generate the phylogenetic trees based on distance analysis for 16S rRNA and functional genes, respectively. To estimate the robustness of inferred topologies and the reproducibility of the trees, 1,000 bootstrap re-sampling was tested using the same distance model.

## Nucleotide Sequence Accession Numbers

The nucleotide sequences have been submitted in the DDBJ/EMBL/GenBank databases under accession numbers: MF624634 to MF624712 for the archaeal and bacterial 16S rRNA gene sequences, MF662830 to MF662891 for the thaumarchaeal *amoA* gene sequence, MF662892 to MF662967 for the thaumarchaeal *hbd* gene sequences.

## RESULTS AND DISCUSSION

### Latitudinal and Vertical Trends of Prokaryotic Parameters in the Deep Mediterranean Sea

Spatial patterns of relevant physical variables, as well as prokaryotic parameters (PHP, PR, PGE) and contribution of ABD to prokaryotic carbon demand, measured along the longitudinal gradient of the Mediterranean Sea, are reported in **Table 2** as the mean values and the range of standard deviations. Hydrographical data revealed that the Atlantic station (ST1) was characterized by colder and lower salinity water masses. As a consequence, all prokaryotic parameters measured at ST1 below 750 m were among the lowest (**Table 2**). When considering the seven stations sampled, the total prokaryotic abundance decreased significantly with depth ( $p < 0.001$ ). Moreover, as the second commonly reported pattern, the prokaryotic abundance was observed to be slightly higher in the Algero-Balear sub-basin, compared with the rest of the deep Mediterranean Sea (Two Way ANOVA  $p = 0.005$  or  $p < 0.001$  using geographic location or depth as a factor, respectively). Prokaryotic respiration rates measured with the ETS method did exhibit evident downward-decreasing trend ( $p < 0.05$ ) although they were apparently uniform in both Mediterranean Sea basins. The prokaryotic heterotrophic production (PHP) showed the fastest rates in the eastern basin (ST7) with the maximum values, detected in the deepest layers ( $125.3 \pm 4.5$  and  $97.7 \pm 7.4 \mu\text{g C m}^{-3} \text{d}^{-1}$  at depth of 3,000 m and 4,000 m, respectively). Noteworthy, the PHP rates measured in bathypelagic water masses at majority of locations (ST2-5 and ST7) were significantly higher ( $p < 0.001$ ) than in corresponding mesopelagic compartments (**Table 2**). The highest difference was observed at station ST3, where the heterotrophic production measured at depth of 2,837 m was more than three times higher ( $97.4 \pm 1.9 \mu\text{g C m}^{-3} \text{d}^{-1}$ ) than uppermost PHP values ( $28.6 \pm 0.6 \mu\text{g C m}^{-3} \text{d}^{-1}$ ). Our calculated PGE values (0.3–16%) were similar to the estimates previously calculated for similar areas (Azzaro et al., 2012; Celussi et al., 2017), substantiating the correctness of the conversion factors used in present study. Thus, taken together all aforementioned measurements, which are coincidental with previously reported data (La Ferla et al., 2010; Zaccone et al., 2010, 2012; Luna et al., 2012; Caruso et al., 2013; Celussi et al., 2017), we found that the deep Mediterranean Sea did possess neither the eastward- nor downward-decreasing gradient of main prokaryotic parameters, characteristic for sunlit layers of the Mediterranean Sea (Sarmiento et al., 1988; Danovaro et al., 1999; Thingstad et al., 2005; López-Sandoval et al., 2011).

**TABLE 2 |** Average water masses properties of selected physicochemical and biological parameters in the western, central and eastern Mediterranean sub-basins.

| Variables (m)                      | Salinity | Temp. (°C) | PHP <sup>a</sup> | SD, n = 3 | PR <sup>a</sup> | SD, n = 2 | ABD <sup>a</sup> | SD, n = 3       |
|------------------------------------|----------|------------|------------------|-----------|-----------------|-----------|------------------|-----------------|
| <b>STATION ST1, BOTTOM 2,735 m</b> |          |            |                  |           |                 |           |                  |                 |
| 200                                | 36.01    | 14.13      | 19.4             | 0.8       | 967             | 51        | 394              | 39              |
| 750                                | 36.06    | 11.69      | 11.0             | 0.4       | 987             | 45        | 347              | 27              |
| 2,000                              | 35.17    | 4.58       | 7.7              | 0.0       | 377             | 19        | 0.40             | 0.01            |
| 2,728                              | 34.97    | 3.10       | 5.5              | 0.0       | 204             | 8         | 4.4              | 0.4             |
| <b>STATION ST2, BOTTOM 2,640 m</b> |          |            |                  |           |                 |           |                  |                 |
| 200                                | 38.41    | 13.18      | 34.6             | 1.1       | 1,079           | 54        | 268              | 33              |
| 400                                | 38.53    | 13.24      | ND               | ND        | 794             | 35        | 198              | 24              |
| 1,500                              | 38.47    | 13.08      | 12.5             | 0.3       | 763             | 39        | 204              | 26              |
| 2,633                              | 38.48    | 13.27      | 38.9             | 0.7       | 733             | 22        | 142              | 16              |
| <b>STATION ST3, BOTTOM 2,853 m</b> |          |            |                  |           |                 |           |                  |                 |
| 200                                | 38.30    | 13.52      | 28.6             | 0.6       | 763             | 28        | 250              | 20              |
| 400                                | 38.60    | 13.56      | 8.2              | 0.6       | 946             | 46        | 210              | 11              |
| 1,500                              | 38.47    | 13.08      | 13.7             | 0.1       | 631             | 31        | 240              | 14              |
| 2,837                              | 38.49    | 13.31      | 97.4             | 1.9       | 651             | 17        | 281              | 18              |
| <b>STATION ST4, BOTTOM 3,571 m</b> |          |            |                  |           |                 |           |                  |                 |
| 200                                | 38.64    | 14.04      | 5.5              | 0.1       | 1,577           | 99        | 114              | 14              |
| 400                                | 38.74    | 14.05      | 3.8              | 0.1       | 366             | 13        | 231              | 21              |
| 2,500                              | 38.52    | 13.43      | 5.5              | 0.1       | 753             | 37        | 59               | 9               |
| 3,500                              | 38.50    | 13.56      | 27.8             | 0.5       | 926             | 39        | 48               | 6               |
| <b>STATION ST5, BOTTOM 3,675 m</b> |          |            |                  |           |                 |           |                  |                 |
| 200                                | 38.94    | 14.81      | 23.0             | 0.2       | 794             | 41        | 411              | 31              |
| 400                                | 38.84    | 14.13      | 7.0              | 0.1       | 662             | 34        | 215              | 27              |
| 1,500                              | 38.75    | 13.79      | 5.5              | 0.1       | 662             | 17        | 200              | 11              |
| 2,000                              | 38.74    | 13.80      | 64.6             | 2.8       | 550             | 21        | 249              | 16              |
| 3,000                              | 38.74    | 13.91      | 44.4             | 1.9       | 672             | 17        | 312              | 31              |
| 3,655                              | 38.74    | 13.94      | 37.0             | 3.0       | 712             | 26        | 248              | 21              |
| <b>STATION ST6, BOTTOM 3,625 m</b> |          |            |                  |           |                 |           |                  |                 |
| 200                                | 38.92    | 14.77      | 12.7             | 0.7       | 1,761           | 75        | 140              | 16              |
| 500                                | 38.85    | 14.13      | 13.0             | 0.5       | 662             | 16        | 370              | 36              |
| 1,000                              | 38.75    | 13.74      | 4.8              | 0.1       | 641             | 32        | 290              | 20              |
| 2,000                              | 38.75    | 13.84      | 8.9              | 0.2       | 539             | 19        | 245              | 14              |
| 3,000                              | 38.74    | 13.94      | 6.7              | 0.1       | 570             | 13        | 207              | 19              |
| 3,400                              | 38.74    | 13.94      | ND               | ND        | ND              | ND        | 730 <sup>b</sup> | 41 <sup>b</sup> |
| <b>STATION ST7, BOTTOM 4,346 m</b> |          |            |                  |           |                 |           |                  |                 |
| 200                                | 39.17    | 17.80      | 89.0             | 4.1       | 1,333           | 69        | 160              | 21              |
| 750                                | 38.89    | 14.36      | 33.1             | 0.8       | 814             | 42        | 133              | 14              |
| 1,500                              | 38.77    | 13.88      | 34.3             | 0.9       | 1048            | 41        | 207              | 16              |
| 2,000                              | 38.76    | 13.85      | 81.8             | 4.1       | 590             | 18        | 126              | 10              |
| 3,000                              | 38.77    | 14.08      | 125.3            | 4.5       | 662             | 16        | 143              | 6               |
| 4,000                              | 38.76    | 14.20      | 97.7             | 7.4       | 773             | 35        | 163              | 11              |

<sup>a</sup>Values of prokaryotic heterotrophic production (PHP), prokaryotic respiration (PR) and assimilation of bicarbonate in the dark (ABD) are given in  $\mu\text{g C m}^{-3} \text{d}^{-1}$ .

<sup>b</sup>Data from Yakimov et al. (2007).

ND, not determined.

### Spatial Patterns of ABD in the Deep Mediterranean Sea

Using several molecular and cultivation techniques (Herndl et al., 2005; Kirchman et al., 2007; Grote et al., 2008; Varela et al., 2011; Yakimov et al., 2014), it is now confirmed that DIC fixation

is widespread among prokaryotic organisms in meso- and bathypelagic oceanic water column, including the Mediterranean Sea. It is important to point out that methodology applied through our [ $^{14}\text{C}$ ]-bicarbonate assimilation experiments implied to measure only the [ $^{14}\text{C}$ ]-incorporation into biomass remained after filtration, i.e., to measure rates of the particulate ABD. Thus, the eventual formation of the dissolved radiolabeled compounds, like released organic molecules, extracellular vesicles, signaling devices and enzymes or cellular constituents released after viral lyses (Celussi et al., 2017), was overlooked in present study. Nevertheless, our ABD data were coherent with PHP values, since the last measurement was also ignoring the formation of [ $^3\text{H}$ ]-radiolabeled compounds and cellular constituents, not settled during micro-centrifugation. Deep Mediterranean is very unique basin in a variety of ecological settings. Besides warm temperature and oligotrophy, the concentration of DIC in Mediterranean is very high and ranges from 2.19 to 2.47 mmol  $\text{l}^{-1}$  (Hassoun et al., 2015), compared to 1.72 mmol  $\text{l}^{-1}$  in reference composition of oceanic water with salinity of 35.1‰. Such a high concentration of ambient cold [ $^{12}\text{C}$ ]-bicarbonate obviously affect the specific uptake of added isotopic hot [ $^{14}\text{C}$ ]-bicarbonate (4.464  $\mu\text{mol L}^{-1}$  of this isotope is typically used for DIC fixation experiments). Compared to the isotopic dilution of hot [ $^3\text{H}$ ]-leucine, used throughout present study (mean  $\text{ID} = 1.28$ ), the  $\text{ID}$  values of added [ $^{14}\text{C}$ ]-bicarbonate are in range between 490.6 and 553.3. Thus, to obtain reliable results of ABD, we followed the common practice (Herndl et al., 2005; Reinthaler et al., 2010; Celussi et al., 2017) and increased the volume of sample and prolonged the incubation time with hot [ $^{14}\text{C}$ ]-bicarbonate. However, these different incubation times in PHP and ABD measurements did not pose a problem since it has been shown that leucine uptake rates as well as the bicarbonate assimilation in deep waters are linear over a period of at least 72 h (Reinthaler et al., 2006, 2010; Yakimov et al., 2014).

The westernmost Atlantic station ST1, taken for comparative reasons, was characterized by cold waters below 750 m (4.6 and 3.1°C at 2,000 m and 2,728 m depth, respectively). As a consequence, the ABD values, representing the *dark ocean primary production* rates (term coined by Herndl et al., 2005), decreased from 350 to 400  $\mu\text{g C m}^{-3} \text{d}^{-1}$  at 200–750 m depths to 0.4–4.4  $\mu\text{g C m}^{-3} \text{d}^{-1}$  at ST1 bathypelagic levels (Figure 1 and Table 2). These rates corresponded well to the DIC fixation rates reported for the deep North Atlantic's interior (120 and 1.0  $\mu\text{g C m}^{-3} \text{d}^{-1}$  for the corresponding depths) (Reinthaler et al., 2010). The ABD values measured in dark Mediterranean Sea, unlike those of the Atlantic station ST1, did not evidently exhibit either latitudinal or vertical spatial gradients on average (Two Way ANOVA  $p = 0.629$  or  $p = 0.541$  using depth or geographic location as a factor, respectively; see Figure 1). Station ST4 (Tyrrhenian Sea), represented the single exception, with ABD rates dropping from  $231 \pm 21$  to  $48 \pm 6 \mu\text{g C m}^{-3} \text{d}^{-1}$ , ( $p = 0.006$ ) detected in meso- and bathypelagic waters, respectively. As we discussed it already (Yakimov et al., 2011), earlier estimates of bathypelagic ABD activity (Tamburini et al., 2009) measured in this area at the depth of 3,000 m ( $72.0 \pm 8.9 \mu\text{g C m}^{-3} \text{d}^{-1}$ ) coincided with our values and seem to be a characteristic feature of Tyrrhenian Deep Waters, which are the

oldest, highly oligotrophic and densest deep water masses of the Mediterranean Sea (Millot et al., 2006).

In general, observed uniformity of microbial ABD rates over the 2,500-km-long transect is likely supported by the relative homogeneity of environmental parameters, fundamental for DIC fixation. Indeed, as it reported elsewhere (Danovaro et al., 1999; Yakimov et al., 2011; Santinelli et al., 2015; Celussi et al., 2017 and references herein), the whole Mediterranean interior, from roughly 300–500 m to the seabed, possesses basin-scale minor variations in salinity (<4%), ammonia (<8%), oxygen (<24%), bicarbonate concentrations (<15%), DOC (<10%) and, especially, temperature (<12%). Thus, such evenly distribution of basic environmental settings defines the deep Mediterranean ecosystem as relatively homogenous primarily-producing environment. Documented “hotspots” of autotrophic activity in deep Mediterranean take place at very specific areas, such as deep anoxic hypersaline lakes of Ionian Sea, the large hydrological formations, characterized by the existence of energetically-rich redoxclines (Yakimov et al., 2007, 2013, 2015).

## ABD Rates at the Surficial Layers of Deep Hypersaline Anoxic Lakes

During MICRODEEP2012 and SALINE2014 cruises we measured the ABD values at the interfaces of the deep-sea anoxic hypersaline lakes *Discovery*, *Kryos*, and *Urania*. In our previous studies we demonstrated that these interfaces represent gradients of physical and chemical factors, which constitute major forces shaping active chemoautotrophic ecosystems (Yakimov et al., 2015 and reference therein). Indeed, very fast bicarbonate assimilation rate ( $3.78 \pm 0.57 \text{ mg C m}^{-3} \text{d}^{-1}$ ) has been detected at the upper layer of the NaCl-saturated DHAL *Urania* (Figure 2), comparable with our previous measurements performed on the other thalassohaline DHAL, *L'Atalante* and *Thetis* (Yakimov et al., 2007; La Cono et al., 2011). The lake *Medee*, while exhibiting relatively low ABD rates in the interface ( $1.21 \pm 0.11 \text{ mg C m}^{-3} \text{d}^{-1}$ ), singularly possesses a very thick and active transition zone ( $\sim 40 \text{ m}$ ,  $0.66 \pm 0.06 \text{ mg C m}^{-3} \text{d}^{-1}$ ). The DHAL *Discovery* and *Kryos* are saturated with  $\text{MgCl}_2$  ( $\sim 5\text{M}$ ) and represent the exceptionally chaotropic system with the lowest water activity value registered for any hydrological formation on our planet (Hallsworth et al., 2007; Yakimov et al., 2015). Due to this fact, the ABD values in the *Discovery* and *Kryos* interfaces are significantly lower, compared to that of the thalassohaline DHAL. But these rates are still considerably higher the mean value of DIC fixation rates, measured in the deep Ionian Sea. Using the ABD values calculated for the lake *Medee*, which spans over  $\sim 100 \text{ km}^2$  (Yakimov et al., 2013), net  $\text{CO}_2$  assimilation activities were estimated as  $27.4 \pm 2.5$  tons daily. Hence, the deep brine lakes represent the hotspot of both metabolic activity and microbial diversity and contribute to the global  $\text{CO}_2$  sink in the deep Ionian Sea.

## Importance of ABD in the Mediterranean Interior

According to the literature, the Mediterranean Sea is characterized by clear longitudinal patterns as to the “solar

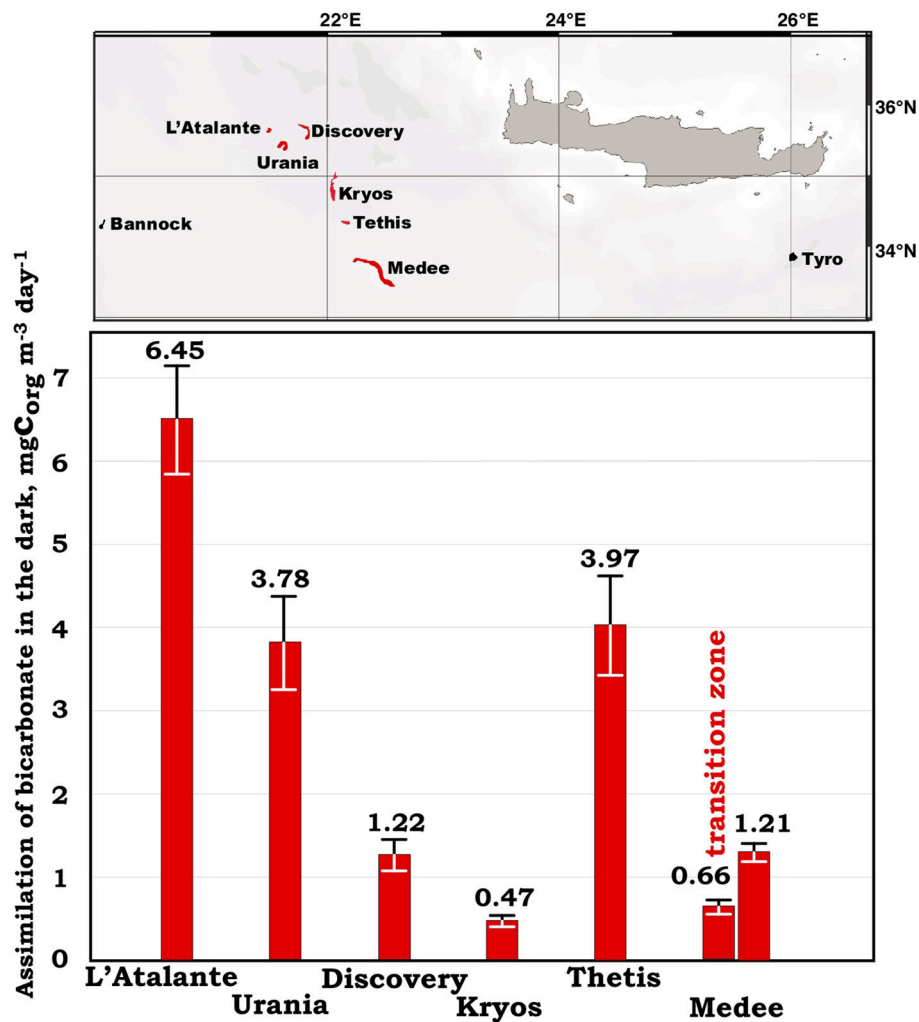


**FIGURE 2** | Location of all currently known Mediterranean DHAL and dark primary production (ABD) rates, measured in oxic/anoxic surficial layer of these deep-sea lakes.

radiation related features.” In particular, together with a deepening of the photic zone lower limit (from 70 to 110 m below the sea surface), it shows decreasing trends of phototrophic primary productivity (PhPP) eastward (Moutin and Raimbault, 2002; Siokou-Frangou et al., 2010; López-Sandoval et al., 2011). In order to compare ABD with phototrophic primary production along the sampled longitudinal transect, we uniformed and averaged the PhPP values, estimated *in situ* and originally obtained from the literature (Moutin and Raimbault, 2002; Siokou-Frangou et al., 2010), for each area, corresponded to Mediterranean stations ST2-ST7 (Table 3). Additionally to these data, the integrated net PhPP values, deduced from the 3-D-biogeochemical OPATM-BFM modeling approach (Lazzari et al., 2012), were also taken into consideration. Depth-integrated ABD assimilation rates in the Mediterranean deep waters ranged from  $396 \pm 49$  (station ST4) to  $873 \pm 99$  mg C m<sup>-2</sup> d<sup>-1</sup> (Table 3). Unlike the west-east decreasing trend in the integrated net phytoplankton primary production, the

ABD rates showed centripetal increase trends, with peaks of ABD activity observed in the central stations ST5 and ST6 (mean value for ST5+ST6:  $867$  mg C m<sup>-2</sup> d<sup>-1</sup>). This may result from at least two reasons. Although the ST2 and ST3 stations of the Western Mediterranean possess the ABD activity (mean value is  $224 \pm 25$  μg C m<sup>-3</sup> d<sup>-1</sup>), similar to that of the central stations ST5 and ST6 (mean value is  $262 \pm 33$  μg C m<sup>-3</sup> d<sup>-1</sup>), this region is considerably shallower. Secondly, the effects of the nearby processes of dense water formation with participation of nutrients-rich Adriatic waters (Korlević et al., 2015) and ammonium- and reductants-rich DHAL most likely define elevated ABD activities, compared to extremely oligotrophic Levantine sub-basin. In conclusion, the measured ABD rates in the Mediterranean Sea accounts for 85–424% of the phototrophic primary production (Table 3), thus clearly highlighting the significance of dark DIC fixation to support meso- and bathypelagic carbon demand. Indeed, the mean ratio of ABD: prokaryotic carbon demand (PCD = PHP + PR) ranged



**TABLE 3** | Regional averages of integrated net phototrophic primary production (PhPP), reported for Mediterranean Sea, and ABD rates, estimated in present study.

| Sub-basin        | Net PhPP rates ( $\text{mg C m}^{-2} \text{d}^{-1}$ ) |                              | Net ABD rates ( $\text{mg C m}^{-2} \text{d}^{-1}$ ) <sup>c</sup> |
|------------------|---|------------------------------|---|
|                  | <i>In situ</i> <sup>14</sup> C <sup>a</sup>           | OPATM-BFM <sup>b</sup> model |   |
| Alboran Sea      | 448 ± 188   | 545 ± 321                    | 465 ± 71 (ST2)  |
| Catalan Balearic | 533 ± 367   | 509 ± 199                    | 645 ± 48 (ST3)  |
| Tyrrhenian Sea   | 367 ± 83  | 279 ± 118                    | 396 ± 49 (ST4)  |
| Ionian Sea       | 324 ± 126   | 189 ± 99                     | 873 ± 99 (ST5)  |
|                  |   |                              | 864 ± 89 (ST6)  |
| Levantine        | 149 ± 80  | 208 ± 110                    | 632 ± 61 (ST7)  |

<sup>a</sup>Data from Siokou-Frangou et al. (2010).

<sup>b</sup>Data from Lazzari et al. (2012).

<sup>c</sup>Average of integrated ABD rates at the ST2-ST7 stations, estimated in present study.

from 5 to 62% (Figure 1 and Table 2). Thus, along the latitudinal transect, most of deep Mediterranean aphotic waters exhibited capacity to self-compensate their PCD on 20–50% by *de novo* production organic carbon in the dark.

Although it was not the objective of the present study, we are aware that decompression of the samples retrieved from greater depth might influence prokaryotic activities, measured at ambient pressure. Since we obtained even distribution of both prokaryotic growth yields and ABD rates in meso- and bathypelagic waters, this would indicate that both production/respiration and assimilation of bicarbonate responded similarly. Whether decompression stimulates or affects the biological activities of deep-sea prokaryotes is still unclear and contradictory (Tamburini et al., 2013 and references therein). Indeed, stimulation of deep water prokaryotic activity was reported in some studies (Jannasch and Wirsén, 1982), while other authors detected inhibition of activity because of decompression (Tamburini et al., 2003, 2009). Thus, lack of general consensus about the pressurized vs. decompressed metabolic activities of deep-sea microbiota yet has to be resolved. Despite of these and other uncertainties, related to the conversion factors and activity calculations, the deep Mediterranean Sea seems significantly contribute to *de novo* production of organic matter and to the global carbon cycling in the basin. This is likely the result of combination of several unique characteristics of Mediterranean Sea, such as high abyssal temperature and the ultra-oligotrophy of the Central-Eastern region (Thingstad et al., 2005).

## Cell-Specific Prokaryotic Carbon Demand and ABD Rates

Over the 2,500-km-long transect, the bicarbonate assimilation rates measured in all our samples, apart of the very active samples collected over the DHAL, ranged from  $48 \pm 6$  to  $411 \pm 31 \mu\text{g C m}^{-3} \text{d}^{-1}$  (Figure 1 and Table 2). These data coincided with our previous measurements, performed in the Tyrrhenian and Ionian Sea (Yakimov et al., 2007, 2011, 2014; Smedile et al., 2013). Besides these measurements, there are very few data available for dark DIC fixation in deep Mediterranean waters.

They demonstrated remarkable discrepancy spanning from 50 to  $7,350 \mu\text{g C m}^{-3} \text{d}^{-1}$  (Tamburini et al., 2009; Celussi et al., 2017). The fastest ABD uptake rates, measured by Celussi et al. (2017) in the Algero-Balear and Levantine sub-basins ( $7.35$  and  $3.85 \text{ mg C m}^{-3} \text{d}^{-1}$ , respectively) are only comparable to our data measured in the upper horizon of DHAL (Figure 2). It is important to remark, as the elevated concentrations of reduced compounds (mainly hydrogen sulfide), originated from lake's anoxic interior, can likely fuel such a high activity of dark DIC fixation in the DHAL interfaces. In contrary, the energy sources for  $\text{CO}_2$ -assimilating microbes in the oxygenated aphotic water column are scanty and hardly sufficient to support the same rates of primary production. Elucidating this question, we analyzed in more details the cell-specific prokaryotic carbon demand (csPCD) and the cell-specific assimilation of bicarbonate in the dark (csABD).

Although prokaryotic abundance decreased exponentially with the depth, both csPCD and csABD showed opposite changes and the cell-specific values significantly increased toward the deeper water masses ( $r = 0.958$ ,  $p < 0.04$  for the western and  $r = 0.935$ ,  $p < 0.001$  for the eastern sub-basins). With only one exception of cold deep Atlantic waters (ST1), the highest csPCD and csABD rates were measured at the greatest depths (Table 4). In all studied stations of the Mediterranean basin, the cell-specific PCD values ranged from  $1.72 \pm 0.15 \text{ fg C cell}^{-1} \text{d}^{-1}$  (200 m depth, station ST3) to  $19.87 \pm 2.48 \text{ fg C cell}^{-1} \text{d}^{-1}$  (3,500 m depth, station ST4). These results are similar to previous oceanographic studies, where the cell-specific PCD values of 8–36  $\text{fg C cell}^{-1} \text{d}^{-1}$  were reported (Reinthal et al., 2006). Compared to the csPCD, the cell-specific ABD rates were more homogenous in whole aphotic Mediterranean and varied between  $0.38 \pm 0.08 \text{ fg C cell}^{-1} \text{d}^{-1}$  (200 m depth, station ST7) and  $3.91 \pm 0.57 \text{ fg C cell}^{-1} \text{d}^{-1}$  (3,500 m depth, station ST6). Taking into account an average of carbon content per cell ( $10\text{--}20 \text{ fg C cell}^{-1}$ ) (Danovaro et al., 2008; Kallmeyer et al., 2012), this assimilation activity could likely support the autotrophic microbial growth with a generation time of 2.5–50 days. As we mentioned above, the planktonic *Thaumarchaeota* belonging to MG1 dominate the prokaryotic cell numbers in ocean interior and seem play an important role in DIC fixation in the aphotic meso- and bathypelagic ocean (Francis et al., 2005; Herndl et al., 2005; Reinthal et al., 2010; Middelburg, 2011; Tolar et al., 2016). Cells of the first cultured representative, “*Candidatus Nitrosopumilus maritimus*” SCM1, are capable to grow autotrophically to a density of  $3 \times 10^7 \text{ cells mL}^{-1}$  ( $\sim 0.6 \mu\text{g mL}^{-1}$  dry mass) with a generation time of 35 h, which requires a carbon-fixation rate of  $39 \text{ nmol d}^{-1} \mu\text{g}^{-1}$  protein (Könneke et al., 2014). As the average of crude protein content in microbial biomass is 40–60% dry weight, these values corresponded to cell-specific fixation rates of  $3.7\text{--}5.6 \text{ fg C cell}^{-1} \text{d}^{-1}$ . Overall, statistical summaries of our csABD data corresponded well with the literature values of microbial cell-specific DIC assimilation, including the data of cultivation trials (Lenk et al., 2011; Swan et al., 2011; Könneke et al., 2014; Yakimov et al., 2014; Dykstra et al., 2016; Cao et al., 2017).

However, it seems that ammonium-oxidizing *Thaumarchaea* are not the only player of ABD in the deep Mediterranean

**TABLE 4 |** Prokaryotic abundance (PA), cell-specific prokaryotic carbon demand (csPCD) and cell-specific assimilation of bicarbonate in the dark (csABD) in the water masses of the Mediterranean sub-basins.

| Variables (m)                      | PA, 10 <sup>3</sup> cell mL <sup>-1</sup> | SD              | csPCD, fg C cell <sup>-1</sup> d <sup>-1</sup> | SD   | csABD, fg C cell <sup>-1</sup> d <sup>-1</sup> | SD    |
|------------------------------------|---|-----------------|--|------|--|-------|
| <b>STATION ST1. BOTTOM 2,735 m</b> |   |                 |  |      |  |       |
| 200                                | 240                                       | 21              | 4.11   | 0.57 | 1.64   | 0.39  |
| 750                                | 180                                       | 8               | 5.54   | 0.49 | 1.93   | 0.24  |
| 2,000                              | 92  | 8               | 4.18   | 0.57 | 0.004  | 0.001 |
| 2,728                              | 75  | 7               | 2.79   | 0.36 | 0.06   | 0.01  |
| <b>STATION ST2. BOTTOM 2,640 m</b> |   |                 |  |      |  |       |
| 200                                | 450                                       | 42              | 2.47   | 0.35 | 0.60   | 0.13  |
| 400                                | 350                                       | 27              | ND   | ND   | 0.57   | 0.12  |
| 1,500                              | 260                                       | 19              | 2.98   | 0.37 | 0.78   | 0.16  |
| 2,633                              | 170                                       | 14              | 4.54   | 0.35 | 0.84   | 0.16  |
| <b>STATION ST3. BOTTOM 2,853 m</b> |   |                 |  |      |  |       |
| 200                                | 460                                       | 24              | 1.72   | 0.15 | 0.54   | 0.07  |
| 400                                | 150                                       | 9               | 6.36   | 0.69 | 1.40   | 0.16  |
| 1,500                              | 220                                       | 11              | 2.93   | 0.29 | 1.09   | 0.11  |
| 2,837                              | 180                                       | 8               | 4.16   | 0.29 | 1.56   | 0.17  |
| <b>STATION ST4. BOTTOM 3571 m</b>  |   |                 |  |      |  |       |
| 200                                | 187                                       | 19              | 8.46   | 1.39 | 0.61   | 0.14  |
| 400                                | 131                                       | 9               | 2.82   | 0.29 | 1.76   | 0.28  |
| 2,500                              | 99  | 7               | 7.66   | 0.91 | 0.60   | 0.13  |
| 3,500                              | 48  | 4               | 19.87  | 2.48 | 1.00   | 0.21  |
| <b>STATION ST5. BOTTOM 3675 m</b>  |   |                 |  |      |  |       |
| 200                                | 170                                       | 13              | 4.81   | 0.60 | 2.42   | 0.37  |
| 400                                | 132                                       | 11              | 5.07   | 0.68 | 1.63   | 0.34  |
| 1,500                              | 122                                       | 11              | 5.47   | 0.63 | 1.64   | 0.24  |
| 2,000                              | 72  | 6               | 8.54   | 1.04 | 3.46   | 0.51  |
| 3,000                              | 84  | 6               | 8.53   | 0.83 | 3.71   | 0.63  |
| 3,655                              | 79  | 9               | 9.48   | 1.44 | 3.14   | 0.62  |
| <b>STATION ST6. BOTTOM 3625 m</b>  |   |                 |  |      |  |       |
| 200                                | 221                                       | 17              | 8.03   | 0.96 | 0.63   | 0.12  |
| 500                                | 140                                       | 8               | 4.82   | 0.39 | 2.64   | 0.41  |
| 1,000                              | 150                                       | 12              | 4.31   | 0.56 | 1.93   | 0.29  |
| 2,000                              | 75  | 5               | 7.31   | 0.74 | 3.27   | 0.40  |
| 3,000                              | 53  | 3               | 10.88  | 0.86 | 3.91   | 0.57  |
| 3,400                              | 1005 <sup>a</sup>                         | 65 <sup>a</sup> | ND   | ND   | 0.73   | 0.09  |
| <b>STATION ST7. BOTTOM 4346 m</b>  |   |                 |  |      |  |       |
| 200                                | 423                                       | 34              | 3.36   | 0.44 | 0.38   | 0.08  |
| 750                                | 218                                       | 13              | 3.89   | 0.42 | 0.61   | 0.1   |
| 1,500                              | 205                                       | 8               | 5.28   | 0.41 | 1.01   | 0.12  |
| 2,000                              | 127                                       | 9               | 5.29   | 0.54 | 0.99   | 0.15  |
| 3,000                              | 136                                       | 16              | 5.79   | 0.83 | 1.05   | 0.17  |
| 4,000                              | 84  | 8               | 10.37  | 1.50 | 1.94   | 0.31  |

<sup>a</sup>Data from Yakimov et al. (2007).

ND, not determined.

(Yakimov et al., 2014 and references herein). Relying on availability of other electron donors (i.e., reduced sulfur intermediates, CO and H<sub>2</sub>), chemolithoauto- and chemoorganotrophic communities, primarily sulfur-oxidizing and carboxydrotrophic bacteria, are capable to perform assimilation of bicarbonate (Swan et al., 2011; Anantharaman

et al., 2013). Additionally, a vast majority of heterotrophic bacteria can incorporate CO<sub>2</sub> using metabolic pathways not necessary related to autotrophy. Depending on organic compounds for carbon supply, these heterotrophic organisms fix carbon dioxide via a variety of carboxylation reactions, including those of anaplerosis (Romanenko, 1964; Hesselsoe et al., 2005, 2008; Alonso-Sáez et al., 2010; Llorós et al., 2011; DeLorenzo et al., 2012; Yakimov et al., 2014). The autotrophic potential in marine mesophilic bacterial isolates is consistent with the CO<sub>2</sub> assimilation activity of “*Candidatus Nitrosopumilus maritimus*” SCM1 and can reach the levels of 0.5–7.5 fg C cell<sup>-1</sup> d<sup>-1</sup> depending on bacterial isolates (Lenk et al., 2011; Yakimov et al., 2014; Dyksma et al., 2016; Cao et al., 2017).

Unlike both these literature values and our calculations, Celussi et al. (2017) reported very high estimates of the MS dark primary production data. Combining estimates of total prokaryotic abundance at bathypelagic (>2,000 m) depths with these ABD data, we assessed that the cell-specific CO<sub>2</sub> fixation rates in this case have to be very high, namely 24–35 fg C cell<sup>-1</sup> d<sup>-1</sup> for bathypelagic water masses of Agero-Balear and Ionian stations and even higher, up to 70 fg C cell<sup>-1</sup> d<sup>-1</sup>, for bathypelagic water masses of Tyrrhenian Sea. Such cell-specific ABD values are considerably different from our data and from those obtained by culturing of CO<sub>2</sub>-fixing isolates in optimized media. At the moment we are at a loss to explain such discrepancy. Obviously, more studies are needed both to unify the measurements of the deep-water DIC fixation rates and to cultivate the key players of this process with the subsequent studies on their ecophysiology.

## Establishment of Actively Nitrifying and CO<sub>2</sub>-Fixing Enrichment Cultures

As we reported previously, the dark CO<sub>2</sub> uptake peaks at the DHAL interfaces coincided with the recovery of metabolically active chemolithoautotrophic *Thaumarchaeota* belonging to MG1 and members of various proteobacterial classes (Yakimov et al., 2007, 2013, 2015; La Cono et al., 2011). As far as these organisms seem to act as the key players in highly active CO<sub>2</sub> fixation processes detected at these depths, the samples of the *LAtalante* and *Kryos* interfaces were used to obtain autotrophic and nitrifying enrichments ATA and KRY. The enrichment SAL5 was established using the bathypelagic sample (3,000 m depth), collected over the brine lake *Urania*. Ammonia consumption in the enrichment cultures was initially observed after 6 months of incubation at 16°C. Consecutive cell passages in NH<sub>4</sub>Cl-containing medium over a period of 2 years resulted in the stably nitrifying ATA, KRY and SAL5 enrichments. Independently on initially added amount, ammonia was completely disappeared in the cultures after 35–40 days of cultivations (data not shown), although no stoichiometric production of nitrite via ammonia oxidation was observed (Figure 3), likely indicating that ammonium was used both in dissimilation and assimilation processes. Specifically, the maximum amount of produced nitrite (384 ± 13 μM) was detected in the ATA enrichment after 35 days of incubation in the dark at 16°C. The SAL5 enrichment, amended with 100 μM NH<sub>4</sub>Cl, converted 84–87% of ammonia

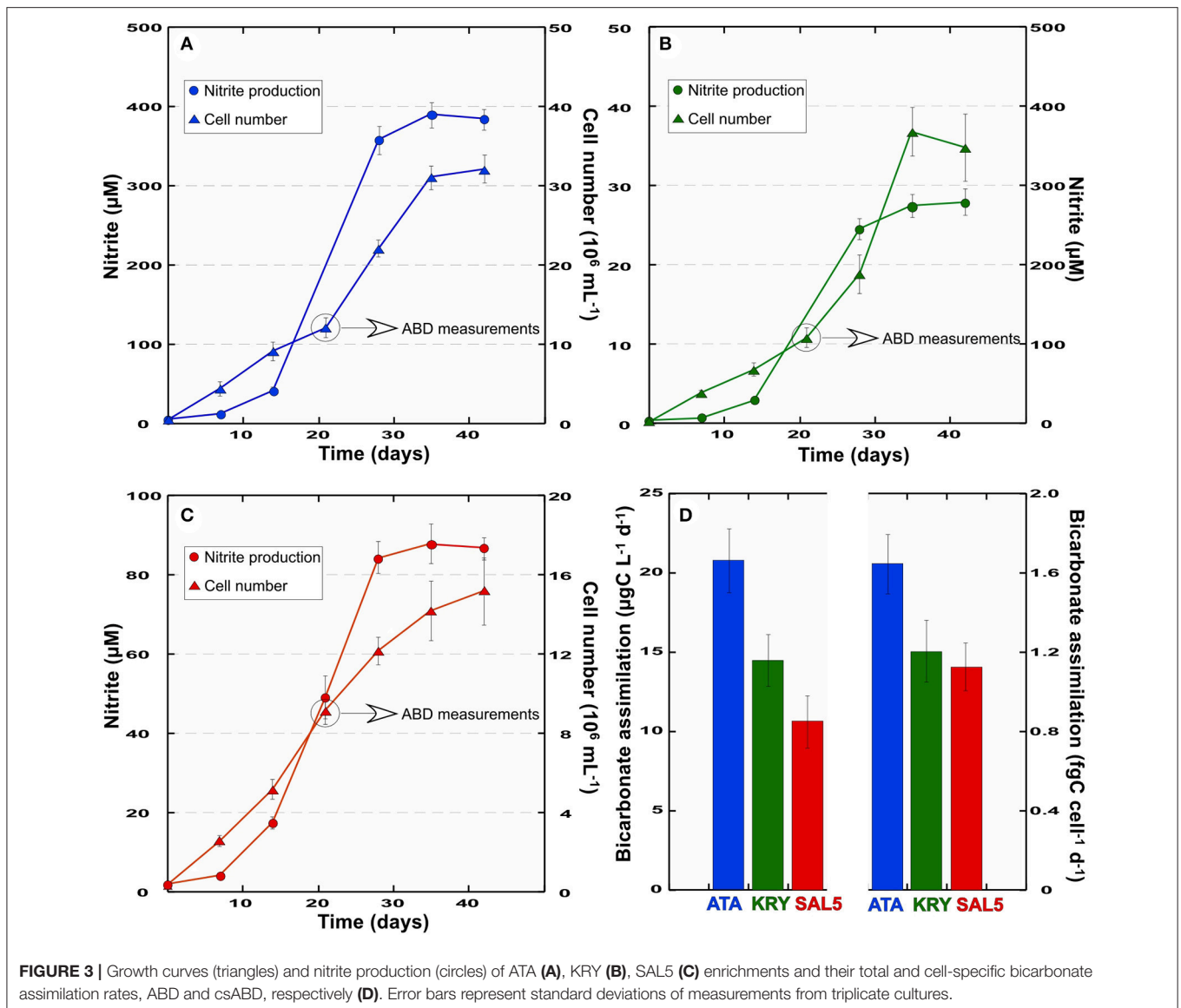


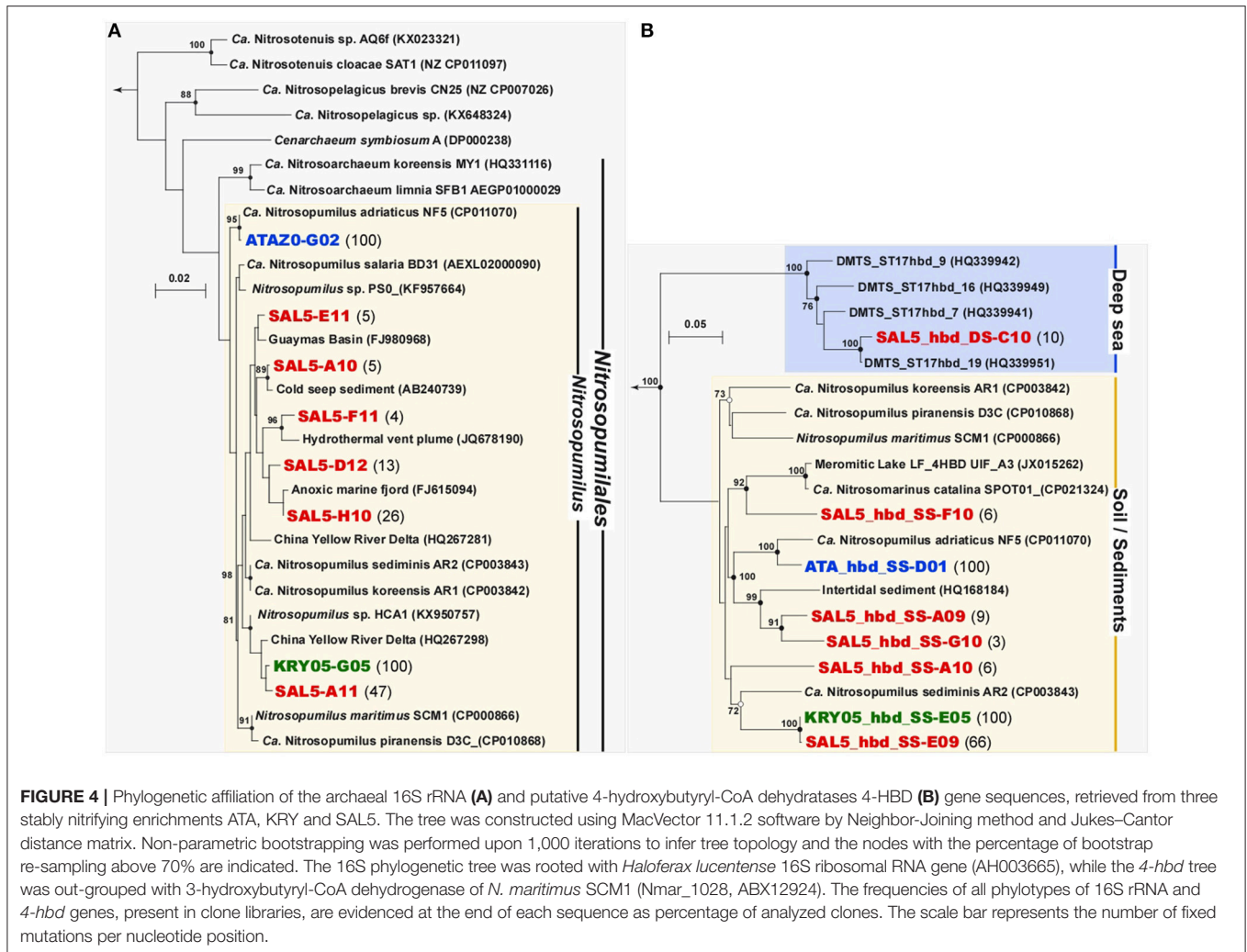
**FIGURE 3** | Growth curves (triangles) and nitrite production (circles) of ATA (A), KRY (B), SAL5 (C) enrichments and their total and cell-specific bicarbonate assimilation rates, ABD and csABD, respectively (D). Error bars represent standard deviations of measurements from triplicate cultures.

after 1 month of cultivation. The KRY enrichment was least active in nitrification and only 56% of available ammonia was converted in nitrite. As far as the scope of the present study was to obtain stable nitrifying and  $\text{CO}_2$ -fixing enrichments, rather than the pure culture of ammonia-oxidizing chemolithotrophs, the presence of ammonia-assimilating bacterial population was not excluded. Hence, eventual heterotrophic members of consortia likely assimilated the residual ammonia. The subsample (5 mL) for the ABD measurements, was taken from the enrichments after 3 weeks of cultivation, which corresponded to a period when one half of the maximum nitrite was produced (Figure 3). Very fast bicarbonate assimilation rate ( $20.7 \pm 1.5 \text{ ng C mL}^{-1} \text{ d}^{-1}$ ) has been detected in the ATA enrichment, which was twice as high the ABD rates, observed in the SAL5 enrichment ( $10.7 \pm 0.9 \text{ ng C mL}^{-1} \text{ d}^{-1}$ ). Daily cellular specific rates of bicarbonate assimilation (csABD) varied depending on enrichments, although in much less extent ( $1.12\text{--}1.64 \text{ fgC cell}^{-1}$

$\text{d}^{-1}$ ). These csABD assimilation activity values, which coincide well with our abovementioned data, confirm the consistency of the present study.

### Phylogenetic Analysis of Archaeal Component in the Enrichment Cultures and Characterization of Ammonia-Oxidizing Archaeal Ecotypes

Phylogenetic analysis of archaeal 16S rRNA clone libraries showed that all three enrichments were consisted exclusively of members of *Thaumarchaeota* Marine Group I.1a (provisional order *Nitrosopumilales*) belonging to the genus *Nitrosopumilus* (Figure 4). Noteworthy, both high ammonium concentration-amended ATA and KRY enrichments were inhabited by two different but monophyletic archaeal cultures. Based on 16S rRNA gene phylogeny, the ATA culture was identical (99.9%) to "*Ca. N.*



adriaticus” NF5, enriched from Northern Adriatic coastal surface waters sampled off Piran (Slovenia) at the depth of 0.5 m (Bayer et al., 2016). Together with environmental clones, recovered worldwide from various coastal marine and estuary sediments, the KRY culture forms a sub-cluster, tightly related (99.2%) to the strain HCA1, enriched from 50 m water from the Puget Sound Regional Synthesis Model (PRISM) Station P10 in Hood Canal (Salish Sea, Pacific Ocean) (Qin et al., 2014). Surprisingly, the total of six *Nitrosopumilus* phylotypes (the similarity cutoff of <99%) were recovered from low ammonia-amended SAL5 enrichment. The most representative phylotype, SAL5\_A11 (47% of all clones sequenced), was almost identical to the KRY culture KRY05-G05 (99.6% of identity), whereas remaining clones were grouped into five distinct groups, recovered from different deep-sea and oxygen-depleted marine ecosystems worldwide without cultivated representatives (Figure 4A).

All *Thaumarchaeota* that have been characterized thus far, possess a modified 3-hydroxypropionate/4-hydroxybutyrate (3HP/4HB) pathway, which has been proposed as the most energy-efficient aerobic pathway for CO<sub>2</sub> fixation (Könneke

et al., 2014). In addition to acetyl-CoA carboxylase, initiating the 3HP/4HB cycle, the second key enzyme, unambiguously indicating the presence of autotrophic 3-HP/4-HB pathway, is the 4-hydroxybutyryl-CoA dehydratase (4-HBD) (Berg et al., 2007, 2010). This FAD- and [4Fe–4S]-containing enzyme, which catalyzes dehydration of 4-hydroxybutyryl-CoA with production of crotonyl-CoA, is very conservative in mesophilic autotrophic *Thaumarchaeota*. Using the primer pair, specifically targeting thaumarchaeal 4-hbd gene sequences (La Cono et al., 2010), we were able to amplify this gene from all enrichment cultures and a total of 32 archaeal hbd gene fragments were cloned and sequenced from each libraries. In strict accordance with observed 16S rRNA gene phylogenetic diversity, both high ammonium-amended enrichments were monophyletic, while SAL5 possessed six distinct phylotypes (Figure 4B). As in the case with 16S rRNA gene, the most representative cluster of SAL5 4-hbd clones (66% of all clones analyzed) were identical to monophyletic KRY phylotype. Noteworthy, the SAL5\_hbd\_DS-C10 phylotype (10% of all clones analyzed) were affiliated with the “Deep-sea Cluster” (Yakimov et al., 2011). Before our study,



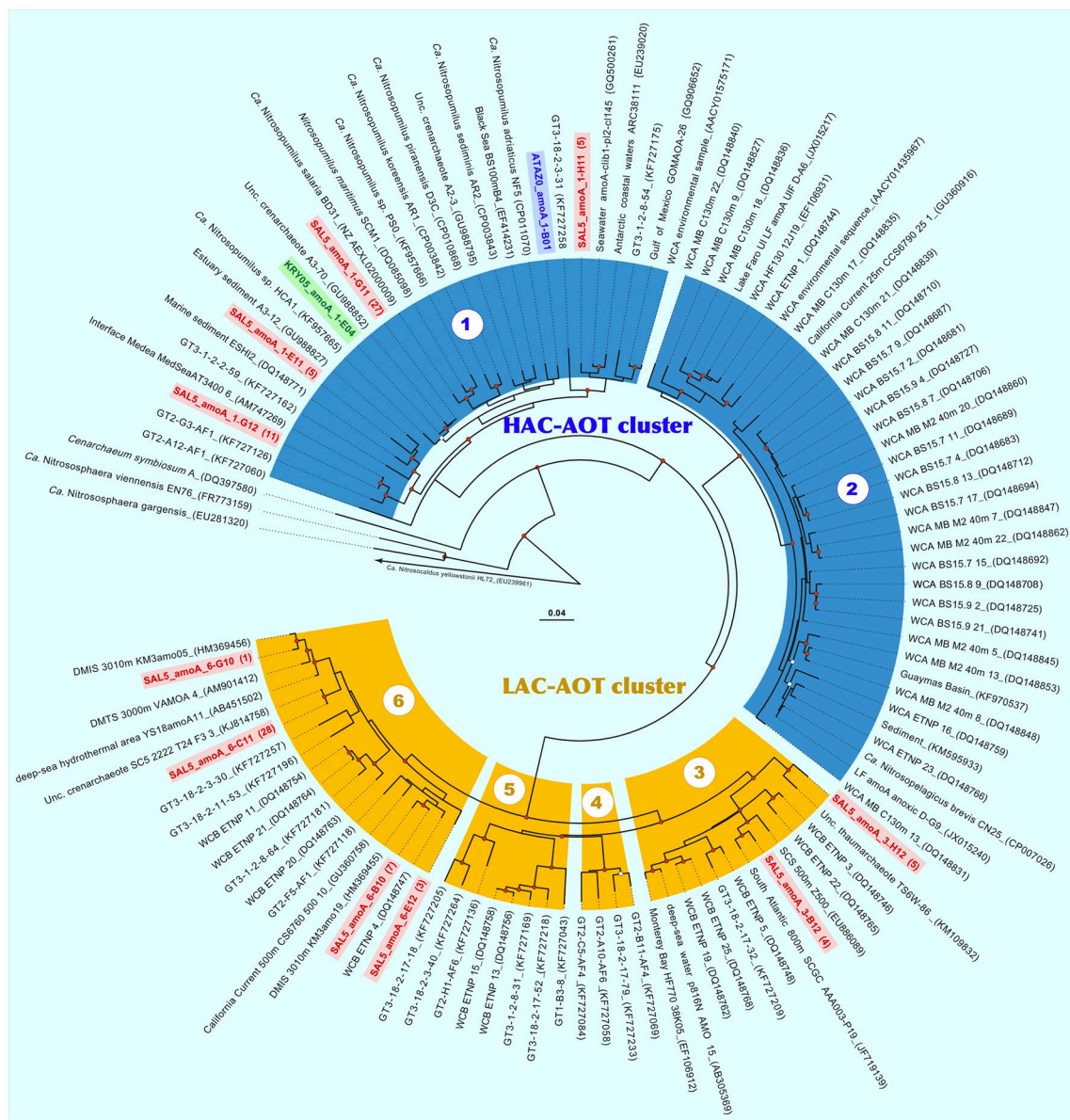


**FIGURE 5 |** Neighbor-joining phylogenetic nucleotide tree of thaumarchaeotal *amoA* obtained from the three stably nitrifying enrichments ATA, KRY, and SAL5. The marine clades 1–2 of high ammonia concentration ammonium-oxidizing archaea (HAC-AOT) and the marine clades 3–6 of low ammonia concentration ammonium-oxidizing archaea (LAC-AOT), as defined by Sintès et al. (2016), are color-coded as aquamarine and yellow, respectively. Sequences of enrichments are also color-coded according to types of clone library origins, as blue (ATA), green (KRY), and red (SAL5). Significant bootstrap values are shown as open (>50) and red-filled (>70) circles at branch nodes.

this cluster, consisting of exclusively bathypelagic sequences, did not possess any cultivated representatives.

Recently, Sintès et al. (2013, 2015, 2016) showed that phylogenetically distinct clusters of marine ammonium-oxidizing thaumarchaea (AOT) inhabit different water layers and regions, which are characterized by various ammonia availability. Consequently, they were divided into the high and low ammonia concentration AOT clusters (HAC- and LAC-AOT). HAC-AOT are dominating in the ocean regions with relatively high ammonia concentrations, like polar and epipelagic waters.

In contrast, LAC-AOT prevail in deep-ocean environments, where ammonia concentrations is often below the detection limit of conventional methods. Following the most relevant classification, all sequences of the marine archaeal *amoA* genes are grouped within six main subclusters (Sintès et al., 2016). Two of them (subclusters 1 and 2) fall into the HAC-AOT cluster and include the sequences from Water Cluster A (WCA) or surface cluster (Francis et al., 2005; Hallam et al., 2006; Mincer et al., 2007). Most epipelagic archaeal *amoA* sequences affiliated to subcluster 2, whereas subcluster 1, which includes *N. maritimus*

SCM1 *amoA*, is more heterogeneous and contains sequences from various marine compartments, including estuaries, lagoons and sediments (Sintes et al., 2016). Four remaining subclusters belong to the LAC-AOT and are dominated by sequences from deep-waters (>200 m depth).

Based on observed diversity of 16S rRNA and *hbd* genes in our enrichments, a total of 32 *amoA* gene fragments were cloned from the ATA and KRY enrichments, while 96 *amoA* clones were analyzed from the SAL5 library. As it was expected from phylogenetic analyses, all ATA and KRY *amoA* sequences were monophyletic and correspondingly affiliated to *Ca. Nitrosopumilus adriaticus* NF5 and *Nitrosopumilus* sp. HCA1 (Figure 5). Diversity of SAL5 *amoA* sequences was much more profound and at least 10 distinct phylotypes (identity cutoff of <97%) were recovered. Noteworthy, only half of SAL5 clones were belonged to subcluster 1 of the HAC cluster, whereas remaining clones were grouping into 6 phylotypes affiliated with members of subclusters 3 (9%) and 6 (41%) of the LAC *amoA* ecotype. Epipelagic HAC and bathypelagic LAC ecotypes of ammonium monooxygenase were recently distinguished at the amino acid level into 38 different oligotypes (Sintes et al., 2016). It has been suggested, that due to the low ammonium concentrations in deep waters, such amino acid substitutions in the AmoA monooxygenase might lead to various adaptive responses: (i) to increase in affinity toward the substrate; (ii) to broaden the spectrum of available substrates; or (iii) to the complete loss of the enzymatic activity due to a lower impact of ammonia oxidation on the *Thaumarchaeota* fitness in ammonium-impoverished environment. Using this classification, we confirmed that together with AmoA of *Nitrosopumilus* sp. HCA1 both KRY and two SAL5 phylotypes belonged to oligotype 12, while remaining phylotypes of HAC-*amoA* cluster (ATAZ0-1 and SAL5-1-G11) possessed novel amino acids combinations, unassigned to any of previously known oligotypes (Table S2). Among the LAC phylotypes, retrieved from SAL enrichment, the aa substitution SAL5-4-H12 was also coined as a novel oligotype. Noteworthy, only thaumarchaeotal representatives of the HAC-AmoA cluster have been enriched or isolated so far (Könneke et al., 2005; Santoro and Casciotti, 2011; Park et al., 2014; Qin et al., 2014; Santoro et al., 2015; Bayer et al., 2016), and it was indicated that more emphasis should be put on offering more realistic ammonium concentrations in culturing approaches than done hitherto (Sintes et al., 2016). Here, for the first time, we demonstrated that members of the LAC ecotype, adapted to low ammonia concentrations, can be obtained in laboratory and maintained as stable enrichments supplemented with 100  $\mu$ M  $\text{NH}_4\text{Cl}$ .

## Phylogenetic Analysis of Bacterial Component in the Enrichment Cultures

Recent studies on DIC assimilation in aphotic ocean reveal a surprising diversity of marine bacteria actively performing this process (Varela et al., 2008; Alonso-Sáez et al., 2010; Lenk et al., 2011; Llíros et al., 2011; DeLorenzo et al., 2012; Yakimov et al., 2014; Dykstra et al., 2016; Cao et al., 2017). Different marine bacterial lineages are capable of DIC

fixation, including putatively heterotrophic taxa of *Alpha*- and *Gammaproteobacteria*, which usually dominated the active DIC-assimilating prokaryoplankton communities worldwide. According to our nitrification assay, the phylogenetic analysis, performed on 96 clones from each library, revealed the co-occurrence in all three nitrifying enrichments of thaumarchaeal population and bacteria exclusively belonging to the *Alpha*- and *Gammaproteobacteria* (Figure 6). Within bacterial clones, the KRY population consisted mainly of the marine genus *Stappia* (75% of the total number of clones). In addition to the *coxL* gene for aerobic CO dehydrogenase, members of this genus often possess *cbbL*, the large subunit gene for ribulose-1,5-bisphosphate carboxylase/oxygenase (RuBisCO form I), suggesting their possibility of lithotrophic or mixotrophic metabolism (Weber and King, 2007). The genes coding for the large subunit of RuBisCO form I were found also in sulfur-oxidizing bacteria of genera *Thiomicrospira* and *Roseovarius*, amounting to 26 and 21% of the total SAL5 and ATA bacterial clones, respectively. The greatest number of SAL5 bacterial clones (56%) were classified within the genus *Marinobacter* known to persist under extremely oligotrophic and nutrient-limited conditions (Riedel et al., 2013) and to

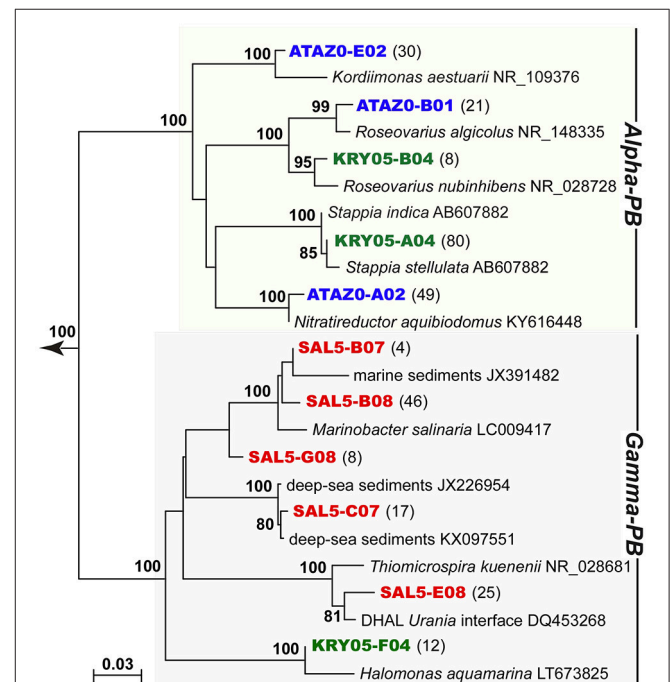


**FIGURE 6** | Phylogenetic affiliation of the bacterial 16S rRNA gene sequences, retrieved from the stably nitrifying enrichments ATA, KRY, and SAL5. The tree was constructed by Neighbor-Joining method and Jukes–Cantor distance matrix using MacVector 11.1.2. Non-parametric bootstrapping was performed upon 1,000 iterations to infer tree topology and the nodes with the percentage of bootstrap re-sampling above 70% are indicated. The 16S phylogenetic tree was rooted with *Sunxiuqinia elliptica* 16S ribosomal RNA gene (GQ200196). The frequencies of all phylotypes of 16S rRNA, present in clone libraries, are evidenced at the end of each sequence as number of corresponding clones, respectively. The scale bar represents the number of fixed mutations per nucleotide position.

possess efficient aerobic denitrification ability (Zheng et al., 2012). Autotrophic denitrification performance was also reported for extremely oligotrophic bacteria belonging to the genus *Nitratireductor* (Nguyen et al., 2015; Park et al., 2017), which was represented by almost half of all ATA clones analyzed. Remaining clones of the ATA library belonged to genus *Kordiimonas*. Similarly to *Marinobacter* and *Nitratireductor*, enrichment and isolation of *Kordiimonas* strains usually require low nutrient media and long incubation periods (Wu et al., 2016). Observed co-occurrence patterns of *Thaumarchaeota* with chemoheterotrophic *Proteobacteria* are in coherence with cultivation and physiological assays recently performed on autotrophic AOT (Beman et al., 2011; Park et al., 2014; Qin et al., 2014; Bayer et al., 2016). It was suggested that in concert, these prokaryotic groups might be involved in the re-mineralization of organic material and hence, nutrient cycling. Additionally, the dependence of autotrophic AOT on small organic molecules as required metabolites provided by bacterial component of consortium cannot be completely excluded.

Taken together, our results provide evidence for complex interactions between various physiological groups of bathypelagic prokaryotes and point toward careful quantification of several key metabolic processes involved in the global carbon cycle/sink in the ocean interior. The long-term bicarbonate-assimilating and nitrifying enrichments, conducted in present study, indicate that both HAC and LAC ecotypes of ammonium-oxidizing *Thaumarchaeota* can co-occur stably with chemoheterotrophic *Proteobacteria*, hence supporting an assumption on their symbiotic interactions in natural environments. Notably, besides the amount of added ammonia, all enrichments were otherwise similarly treated. Nonetheless, the LAC-amended SAL5 enrichment exhibits consistent differences in AOT diversity, compared to the conventionally processed ATA and KRY enrichments. Although with the information available at the moment, we cannot determine

the specific effect of added ammonia (e.g., loss of enzymatic function or eventual toxicity of intermediates), the strong positive selection toward the HAC ecotype in the enrichments, supplemented with 500  $\mu\text{M}$   $\text{NH}_4\text{Cl}$ , might indicate some degree of environmental adaptation leading to niche specialization of these two main ecotypes of AOT. From these data, we can begin to pinpoint genomic adaptations of the ecologically important ubiquitous deep-sea LAC ecotype, and further understand their environmental constraints and metabolic potential.

## AUTHOR CONTRIBUTIONS

VL, LG, and MY conceived the research. VL, GR, FC, and RD did enrichment work. FS, GL, FD, LM, GM, MA, VL, FC, MY did oceanographic work and performed all the data analysis. MY drafted the manuscript, VL, FS, MA, and LG contributed to the manuscript writing.

## ACKNOWLEDGMENTS

We thank the captain and the crew of R/V *Urania* and R/V *Universitatis* for their expert handling of our equipment during the cruise, for highly productive technical assistance and splendid atmosphere on board. This work was done thanks to financial support of the Italian Ministry of University and Research under RITMARE Flagship Project (2012–2016). This research was also supported by “INMARE” Project (Contract H2020-BG-2014-2634486), funded by the European Union’s Horizon 2020 Research Program.

## SUPPLEMENTARY MATERIAL

The Supplementary Material for this article can be found online at: <https://www.frontiersin.org/articles/10.3389/fmicb.2018.00003/full#supplementary-material>

## REFERENCES

- Alonso-Sáez, L., Galand, P. E., Casamayor, E. O., Pedrós-Alió, C., and Bertilsson, S. (2010). High bicarbonate assimilation in the dark by Arctic bacteria. *ISME J.* 4, 1581–1590. doi: 10.1038/ismej.2010.69
- Altschul, S. F., Madden, T. L., Schäffer, A. A., Zhang, J., Zhang, Z., Miller, W., et al. (1997). Gapped BLAST and PSI-BLAST: a new generation of protein database search programs. *Nucleic Acids Res.* 25, 3389–3402. doi: 10.1093/nar/25.17.3389
- Anantharaman, K., Breier, J. A., Sheik, C. S., and Dick, G. J. (2013). Evidence for hydrogen oxidation and metabolic plasticity in widespread deep-sea sulfur-oxidizing bacteria. *Proc. Natl. Acad. Sci. U.S.A.* 110, 330–335. doi: 10.1073/pnas.1215340110
- Aristegui, J., Duarte, C. M., Gasol, J. M., and Alonso-Sáez, L. (2005). Active mesopelagic prokaryotes support high respiration in the subtropical northeast Atlantic Ocean. *Geophys. Res. Lett.* 32:L03608. doi: 10.1029/2004GL021863
- Aristegui, J., Gasol, J. M., Duarte, C. M., and Herndl, G. J. (2009). Microbial oceanography of the dark ocean’s pelagic realm. *Limnol. Oceanogr.* 54, 1501–1529. doi: 10.4319/lo.2009.54.5.1501
- Ashford, K. E., Chuzhanova, N. A., Fry, J. C., Jones, A. J., and Weightman, A. J. (2006). New screening software shows that most recent large 16S rRNA gene clone libraries contain chimeras. *Appl. Environ. Microbiol.* 72, 5734–5741. doi: 10.1128/AEM.00556-06
- Azzaro, M., La Ferla, R., and Azzaro, F. (2006). Microbial respiration in the aphotic zone of the Ross Sea (Antarctica). *Mar. Chem.* 99, 199–209. doi: 10.1016/j.marchem.2005.09.011
- Azzaro, M., La Ferla, R., Maimone, G., Monticelli, L. S., Zaccone, R., and Civitarese, G. (2012). Prokaryotic dynamics and heterotrophic metabolism in a deep convection site of Eastern Mediterranean Sea (the Southern Adriatic Pit). *Continental Shelf Res.* 44, 106–118. doi: 10.1016/j.csr.2011.07.011
- Baltar, F., Aristegui, J., Sintés, E., Van Aken, H. M., Gasol, J. M., and Herndl, G. J. (2009). Prokaryotic extracellular enzymatic activity in relation to biomass production and respiration in the meso- and bathypelagic waters of the (sub)tropical Atlantic. *Environ. Microbiol.* 11, 1998–2014. doi: 10.1111/j.1462-2920.2009.01922.x
- Bayer, B., Vojvoda, J., Offre, P., Alves, R. J., Elisabeth, N. H., Garcia, J. A., et al. (2016). Physiological and genomic characterization of two novel marine thaumarchaeal strains indicates niche differentiation. *ISME J.* 10, 1051–1063. doi: 10.1038/ismej.2015.200
- Beman, J. M., Steele, J. A., and Fuhrman, J. A. (2011). Co-occurrence patterns for abundant marine archaeal and bacterial lineages in the



- deep chlorophyll maximum of coastal California. *ISME J.* 5, 1077–1085. doi: 10.1038/ismej.2010.204
- Berg, I. A., Kockelkom, D., Ramos-Vera, W. H., Say, R. F., Zarzycki, J., Hügler, M., et al. (2010). Autotrophic carbon fixation in archaea. *Nat. Rev. Microbiol.* 8, 447–460. doi: 10.1038/nrmicro2365
- Berg, I. A., Kockelkorn, D., Buckel, W., and Fuchs, G. (2007). A 3-Hydroxypropionate/4-Hydroxybutyrate autotrophic carbon dioxide assimilation pathway in Archaea. *Science* 318, 1782–1786. doi: 10.1126/science.1149976
- Burd, A. B., Hansell, D. A., Steinberg, D. K., Anderson, T. R., Aristegui, J., Baltar, F., et al. (2010). Assessing the apparent imbalance between geochemical and biochemical indicators of meso- and bathypelagic biological activity: what the @!\$#? Is wrong with present calculations of carbon budgets? *Deep-Sea Res. Part II* 57, 1557–1571. doi: 10.1016/j.dsr2.2010.02.022
- Cao, W., Das, A., Saren, G., Jiang, M., Zhang, H., and Yu, X. (2017). Autotrophic potential in mesophilic heterotrophic bacterial isolates from Sino-Pacific marine sediments. *Acta Oceanol. Sin.* 36, 69–77. doi: 10.1007/s13131-016-0962-2
- Carpenter, J. H. (1965). The accuracy of the Winkler method for dissolved oxygen analysis. *Limnol. Oceanogr.* 10, 135–140. doi: 10.4319/lo.1965.10.1.0135
- Caruso, G., Monticelli, L. S., La Ferla, R., Maimone, G., Azzaro, M., Azzaro, F., et al. (2013). Patterns of prokaryotic activities and abundance among the epi-meso and bathypelagic zones of the southern-central Tyrrhenian Sea. *Oceanography* 1:105. doi: 10.4172/ocn.1000105
- Celussi, M., Malfatti, F., Ziveri, P., Gianni, M., and Del Negro, P. (2017). Uptake-release dynamics of the inorganic and organic carbon pool mediated by planktonic prokaryotes in the deep Mediterranean Sea. *Environ. Microbiol.* 19, 1163–1175. doi: 10.1111/1462-2920.13641
- Christensen, J. P., Owens, T. G., Devol, A. H., and Packard, T. T. (1980). Respiration and physiological state in marine bacteria. *Mar. Biol.* 55, 267–276. doi: 10.1007/BF00393779
- Danovaro, R., Dell'Anno, A., Corinaldesi, C., Magagnini, M., Noble, R., Tamburini, C., et al. (2008). Major viral impact on the functioning of benthic deep-sea ecosystems. *Nature* 454, p.1084. doi: 10.1038/nature07268
- Danovaro, R., Dinat, A., Duineveld, G., and Tselepidis, A. (1999). Benthic response to particulate fluxes in different trophic environments: a comparison between the Gulf of Lions-Catalan Sea (western-Mediterranean) and the Cretan Sea (eastern-Mediterranean). *Prog. Oceanogr.* 44, 287–312. doi: 10.1016/S0079-6611(99)00030-0
- Del Giorgio, P. A., and Cole, J. J. (1998). Bacterial growth efficiency in natural aquatic systems. *Ann. Rev. Ecol. Syst.* 29, 503–541. doi: 10.1146/annurev.ecolsys.29.1.503
- DeLorenzo, S., Bräuer, S. L., Edgmont, C. A., Herfort, L., Tebo, B. M., and Zuber, P. (2012). Ubiquitous dissolved inorganic carbon assimilation by marine bacteria in the Pacific Northwest coastal ocean as determined by stable isotope probing. *PLoS ONE* 7:e46695. doi: 10.1371/journal.pone.0046695
- Duarte, C. M., Regaudie-de-Gioux, A., Arrieta, J. M., Delgado-Huertas, A., and Agustí, S. (2013). The oligotrophic ocean is heterotrophic. *Annu. Rev. Mar. Sci.* 5, 551–569. doi: 10.1146/annurev-marine-121211-172337
- Dyksma, S., Bischof, K., Fuchs, B. M., Hoffmann, K., Meier, D., Meyerdierks, A., et al. (2016). Ubiquitous *Gammaproteobacteria* dominate dark carbon fixation in coastal sediments. *ISME J.* 10:1939. doi: 10.1038/ismej.2015.257
- Francis, C. A., Roberts, K. J., Beman, J. M., Santoro, A. E., and Oakley, B. B. (2005). Ubiquity and diversity of ammonia-oxidizing archaea in water columns and sediments of the ocean. *Proc. Natl. Acad. Sci. U.S.A.* 102, 14683–14688. doi: 10.1073/pnas.0506625102
- Glöckner, F. O., Fuchs, B. M., and Amann, R. (1999). Bacterioplankton compositions of lakes and oceans: a first comparison based on fluorescence *in situ* hybridization. *Appl. Environ. Microbiol.* 65, 3721–3726.
- Grasshoff, K., Ehrhardt, M., and Kremling, K. (1999). *Methods of Seawater Analysis, 3rd Edn.* Weinheim: Wiley-VCH Verlag GmbH.
- Grote, J., Günter, J., Labrenz, M., Herndl, G. J., and Jürgens, K. (2008). Epsilonproteobacteria represents the major portion of chemoautotrophic bacteria in sulfidic waters of pelagic redoxclines of the Baltic and Black Seas. *Appl. Environ. Microbiol.* 74, 7546–7551. doi: 10.1128/AEM.01186-08
- Hallam, S. J., Mincer, T. J., Schleper, C., Preston, C. M., Roberts, K., Richardson, P. M., et al. (2006). Pathways of carbon assimilation and ammonia oxidation suggested by environmental genomic analyses of marine Crenarchaeota. *PLoS Biol.* 4:e95. doi: 10.1371/journal.pbio.0040095
- Hallsworth, J. E., Yakimov, M. M., Golyshin, P. N., Gillion, J. L., Auria, D., de Lima, G., et al. (2007). Limits of life in MgCl<sub>2</sub>-containing environments: chaotrichity defines the window. *Environ. Microbiol.* 9, 801–813. doi: 10.1111/j.1462-2920.2006.01212.x
- Hassoun, A. E. R., Gemayel, E., Krasakopoulou, E., Goyet, C., Saab, M. A.-A., Guglielmi, V., et al. (2015). Acidification of the Mediterranean Sea from anthropogenic carbon penetration. *Deep Sea Res. Part I Oceanogr. Res. Pap.* 102, 1–15. doi: 10.1016/j.dsr.2015.04.005
- Herndl, G. J., Reinthaler, T., Teira, E., van Aken, H., Veth, C., Pernthaler, A., et al. (2005). Contribution of Archaea to total prokaryotic production in the deep Atlantic Ocean. *Appl. Environ. Microbiol.* 71, 2303–2309. doi: 10.1128/AEM.71.5.2303-2309.2005
- Hesselsoe, M., Bjerring, M. L., Henriksen, K., Loll, P., and Nielsen, J. L. (2008). Method for measuring substrate preferences by individual members of microbial consortia proposed for bioaugmentation. *Biodegradation* 19, 621–633. doi: 10.1007/s10532-007-9167-x
- Hesselsoe, M., Nielsen, J. L., Roslev, P., and Nielsen, P. H. (2005). Isotope labeling and microautoradiography of active heterotrophic bacteria on the basis of assimilation of <sup>14</sup>CO<sub>2</sub>. *Appl. Environ. Microbiol.* 71, 646–655. doi: 10.1128/AEM.71.2.646-655.2005
- Holmes, R. M., Aminot, A., Kérouel, R., Hooker, B. A., and Peterson, B. J. (1999). A simple and precise method for measuring ammonium in marine and freshwater ecosystems. *Can. J. Fish. Aquat. Sci.* 56, 1801–1808. doi: 10.1139/f99-128
- Hügler, M., and Sievert, S. M. (2010). Beyond the Calvin cycle: autotrophic carbon fixation in the ocean. *Annu. Rev. Mar. Sci.* 3, 261–289. doi: 10.1146/annurev-marine-120709-142712
- Ingalls, A. E., Shah, S. R., Hansman, R. L., Aluwihare, L. I., Santos, G. M., Druffel, E. R., et al. (2006). Quantifying archaeal community autotrophy in the mesopelagic ocean using natural radiocarbon. *Proc. Natl. Acad. Sci. U.S.A.* 103, 6442–6447. doi: 10.1073/pnas.0510157103
- Jannasch, H. J., and Wirsén, C. O. (1982). Microbial activities in undecompressed microbial populations from the deep seawater samples. *Appl. Environ. Microbiol.* 43, 1116–1124.
- Kallmeyer, J., Pockalny, R., Adhikari, R. R., Smith, D. C., and D'Hondt, S. (2012). Global distribution of microbial abundance and biomass in subseafloor sediment. *Proc. Natl. Acad. Sci. U.S.A.* 109, 16213–16216. doi: 10.1073/pnas.1203849109
- Karner, M. B., DeLong, E. F., and Karl, D. M. (2001). Archaeal dominance in the mesopelagic zone of the Pacific Ocean. *Nature* 409, 507–510. doi: 10.1038/35054051
- Kirchman, D. L., Elifantz, H., Dittel, A. I., and Malmstrom, R. R. (2007). Standing stocks and activity of *Archaea* and *Bacteria* in the western Arctic Ocean. *Limnol. Oceanogr.* 52, 495–507. doi: 10.4319/lo.2007.52.2.0495
- Kirchman, D., K'nees, E., and Hodson, R. (1985). Leucine incorporation and its potential as a measure of protein synthesis by bacteria in natural aquatic systems. *Appl. Environ. Microbiol.* 49, 599–607.
- Könneke, M., Bernhard, A. E., de la Torre, J. R., Walker, C. B., Waterbury, J. B., and Stahl, D. A. (2005). Isolation of an autotrophic ammonia-oxidizing marine archaeon. *Nature* 437, 543–546. doi: 10.1038/nature03911
- Könneke, M., Schubert, D. M., Brown, P. C., Hügler, M., Standfest, S., Schwander, T., et al. (2014). Ammonia-oxidizing archaea use the most energy-efficient aerobic pathway for CO<sub>2</sub> fixation. *Proc. Natl. Acad. Sci. U.S.A.* 111, 8239–8244. doi: 10.1073/pnas.1402028111
- Korlević, M., Pop Ristova, P., Garić, R., Amann, R., and Orlić, S. (2015). Bacterial diversity in the South Adriatic Sea during a strong, deep winter convection year. *Appl. Environ. Microbiol.* 81, 1715–1726. doi: 10.1128/AEM.03410-14
- La Cono, V., La Spada, G., Arcadi, E., Placenti, F., Smedile, F., Ruggeri, G., et al. (2013). Partaking of *Archaea* to biogeochemical cycling in oxygen-deficient zones of meromictic saline Lake Faro (Messina, Italy). *Environ. Microbiol.* 15, 1717–1733. doi: 10.1111/1462-2920.12060
- La Cono, V., Smedile, F., Bortoluzzi, G., Arcadi, E., Maimone, G., Messina, E., et al. (2011). Unveiling microbial life in new deep-sea hypersaline Lake *Thetis*. Part I: prokaryotes and environmental settings. *Environ. Microbiol.* 13, 2250–2268. doi: 10.1111/j.1462-2920.2011.02478.x
- La Cono, V., Smedile, F., Ferrer, M., Golyshin, P. N., Giuliano, L., and Yakimov, M. M. (2010). Genomic signatures of fifth autotrophic carbon assimilation



- pathway in bathypelagic *Crenarchaeota*. *Microb. Biotechnol.* 3, 595–606. doi: 10.1111/j.1751-7915.2010.00186.x
- La Cono, V., Smedile, F., La Spada, G., Arcadi, E., Genovese, M., Ruggeri, G., et al. (2015). Shifts in the meso- and bathypelagic archaea communities composition during recovery and short-term handling of decompressed deep-sea samples. *Environ. Microbiol. Rep.* 7, 450–459. doi: 10.1111/1758-2229.12272
- La Ferla, R., Azzaro, F., Azzaro, M., Caruso, G., Decembrini, F., Leonardi, M., et al. (2005). Microbial processes contribution to carbon biogeochemistry in the Mediterranean sea: spatial and temporal scale variability of activities and biomass. *J. Mar. Syst.* 57, 146–166. doi: 10.1016/j.jmarsys.2005.05.001
- La Ferla, R., Azzaro, M., Caruso, G., Monticelli, L. S., Maimone, G., Zaccone, R., et al. (2010). Prokaryotic abundance and heterotrophic metabolism in the deep Mediterranean Sea. *Adv. Oceanogr. Limnol.* 1, 143–166. doi: 10.4081/aio.2010.5298
- La Ferla, R., Azzaro, M., Civitarese, G., and Ribera D'Alcalá, M. (2003). Distribution patterns of carbon oxidation in the Eastern Mediterranean Sea: evidence of changes in remineralization processes. *J. Geophys. Res.* 108, 8111. doi: 10.1029/2002JC001602
- Lazzari, P., Solidoro, C., Ibello, V., Teruzzi, A., Beranger, K., Colella, S., et al. (2012). Seasonal and inter-annual variability of plankton chlorophyll and primary production in the Mediterranean Sea: a modelling approach. *Biogeosciences* 9:217. doi: 10.5194/bg-9-217-2012
- Lenk, S., Arnds, J., Zerjatke, K., Musat, N., Amann, R., and Mußmann, M. (2011). Novel groups of *Gammaproteobacteria* catalyze sulfur oxidation and carbon fixation in a coastal, intertidal sediment. *Environ. Microbiol.* 13, 758–774. doi: 10.1111/j.1462-2920.2010.02380.x
- Llirós, M., Alonso-Sáez, L., Gich, F., Plasencia, A., Auguet, O., Casamayor, E. O., et al. (2011). Active bacteria and archaea cells fixing bicarbonate in the dark along the water column of a stratified eutrophic lagoon. *FEMS Microbiol. Ecol.* 77, 370–384. doi: 10.1111/j.1574-6941.2011.01117.x
- López-Sandoval, D. C., Fernández, A., and Marañón, E. (2011). Dissolved and particulate primary production along a longitudinal gradient in the Mediterranean Sea. *Biogeosci.* 8, 815–825. doi: 10.5194/bg-8-815-2011
- Ludwig, W., Strunk, O., Westram, R., Richter, L., Meier, H., Yadhukumar, B., et al. (2004). ARB: a software environment for sequence data. *Nucleic Acids Res.* 32, 1363–1371. doi: 10.1093/nar/gkh293
- Luna, G. M., Bianchelli, S., Decembrini, F., De Domenico, E., Danovaro, R., and Dell'Anno, A. (2012). The dark portion of the Mediterranean Sea is a bioreactor of organic matter cycling. *Global Biogeochem. Cycles* 26, 1–14. doi: 10.1029/2011GB004168
- Middelburg, J. J. (2011). Chemoautotrophy in the ocean. *Geophys. Res. Lett.* 38:L24604. doi: 10.1029/2011GL049725
- Millot, C., Candela, J., Fuda, J. L., and Tber, Y. (2006). Large warming and salinification of the Mediterranean outflow due to changes in its composition. *Deep Sea Res. Part I* 53, 656–666. doi: 10.1016/j.dsr.2005.12.017
- Mincer, T. J., Church, M. J., Taylor, L. T., Preston, C., Kar, D. M., and DeLong, E. F. (2007). Quantitative distribution of presumptive archaeal and bacterial nitrifiers in Monterey Bay and the North Pacific Subtropical Gyre. *Environ. Microbiol.* 9, 1162–1175. doi: 10.1111/j.1462-2920.2007.01239.x
- Molari, M., Manini, M., and Dell'Anno, A. (2013). Dark inorganic carbon fixation sustains the functioning of benthic deep-sea ecosystems. *Global Biogeochem. Cycles* 27, 212–213. doi: 10.1002/gbc.20030
- Mosier, A. C., Allen, E. E., Kim, M., Ferreira, S., and Francis, C. A. (2012). Genome sequence of “*Candidatus Nitrosopumilus salaria*” BD31, an ammonia-oxidizing archaeon from the San Francisco Bay estuary. *J. Bacteriol.* 194, 2121–2122. doi: 10.1128/JB.00013-12
- Moutin, T., and Raimbault, P. (2002). Primary production, carbon export and nutrients availability in western and eastern Mediterranean Sea in early summer 1996 (MINOS cruise). *J. Mar. Syst.* 33, 273–288. doi: 10.1016/S0924-7963(02)00062-3
- Nguyen, V. K., Hong, S., Park, Y., Jo, K., and Lee, T. (2015). Autotrophic denitrification performance and bacterial community at biocathodes of bioelectrochemical systems with either abiotic or biotic anodes. *J. Biosci. Bioeng.* 119, 180–187. doi: 10.1016/j.jbiosc.2014.06.016
- Packard, T. T., Denis, M., Rodier, M., and Gariel, P. (1988). Deep-ocean metabolic CO<sub>2</sub> production: calculations from ETS activity. *Deep Sea Res.* 35, 371–382. doi: 10.1016/0198-0149(88)90016-7
- Packard, T. T., and Williams, P. J. (1981). Rates of respiratory oxygen consumption and electron transport in surface seawater from the Northwest Atlantic. *Oceanol Acta* 4, 351–358.
- Park, S. J., Ghai, R., Martín-Cuadrado, A. B., Rodríguez-Valera, F., Chung, W. H., Kwon, K., et al. (2014). Genomes of two new ammonia-oxidizing archaea enriched from deep marine sediments. *PLoS ONE* 9:e96449. doi: 10.1371/journal.pone.0096449
- Park, Y., Park, S., Nguyen, V. K., Yu, J., Torres, C. I., Rittmann, B. E., et al. (2017). Complete nitrogen removal by simultaneous nitrification and denitrification in flat-panel air-cathode microbial fuel cells treating domestic wastewater. *Chem. Eng. J.* 316, 673–679. doi: 10.1016/j.cej.2017.02.005
- Pollard, P. C., and Moriarty, D. J. (1984). Validity of the tritiated thymidine methods for estimating bacterial growth rates: measurement of isotope dilution during DNA synthesis. *Appl. Environ. Microbiol.* 48, 1076–1083.
- Pruesse, E., Quast, C., Knittel, K., Fuchs, B. M., Ludwig, W., Peplies, J., et al. (2007). SILVA: a comprehensive online resource for quality checked and aligned ribosomal RNA sequence data compatible with ARB. *Nucleic Acids Res* 35, 7188–7196. doi: 10.1093/nar/gkm864
- Pujo-Pay, M., Conan, P., Oriol, L., Cornet-Barthaux, V., Falco, C., Ghiglione, J.-F., et al. (2011). Integrated survey of elemental stoichiometry (C, N, P) from the western to eastern Mediterranean Sea. *Biogeosciences* 8, 883–899. doi: 10.5194/bg-8-883-2011
- Qin, W., Amin, S. A., Martens-Habben, W., Walker, C. B., Urakawa, H., Devol, A. H., et al. (2014). Marine ammonia-oxidizing archaeal isolates display obligate mixotrophy and wide ecotypic variation. *Proc. Natl. Acad. Sci. U.S.A.* 111, 12504–12509. doi: 10.1073/pnas.1324115111
- Reinthal, T., van Aken, H. M., and Herndl, G. J. (2010). Major contribution of autotrophy to microbial carbon cycling in the deep North Atlantic's interior. *Deep Sea Res. Part II* 57, 1572–1580. doi: 10.1016/j.dsr2.2010.02.023
- Reinthal, T., van Aken, H., Veth, C., Aristegui, J., Robinson, C., Williams, P. J. L., et al. (2006). Prokaryotic respiration and production in the meso- and bathypelagic realm of the eastern and western North Atlantic basin. *Limnol. Oceanogr.* 51, 1262–1273. doi: 10.4319/lo.2006.51.3.1262
- Riedel, T. E., Berelson, W. M., Neelson, K. H., and Finkel, S. E. (2013). Oxygen consumption rates of bacteria under nutrient-limited conditions. *Appl. Environ. Microbiol.* 79, 4921–4931. doi: 10.1128/AEM.00756-13
- Romanenko, V. I. (1964). Heterotrophic assimilation of CO<sub>2</sub> by bacterial flora of water. *Microbiologiya* 33, 610–614.
- Santinelli, C., Follett, C., Retelletti Brogi, S., Xu, L., and Repeta, D. (2015). Carbon isotope measurements reveal unexpected cycling of dissolved organic matter in the deep Mediterranean Sea. *Mar. Chem.* 177, 267–277. doi: 10.1016/j.marchem.2015.06.018
- Santoro, A. E., and Casciotti, K. L. (2011). Enrichment and characterization of ammonia-oxidizing archaea from the open ocean: phylogeny, physiology and stable isotope fractionation. *ISME J.* 5, 1796–1808. doi: 10.1038/ismej.2011.58
- Santoro, A. E., Dupont, C. L., Richter, R. A., Craig, M. T., Carini, P., McIlvin, M. R., et al. (2015). Genomic and proteomic characterization of “*Candidatus Nitrosopelagicus brevis*”: an ammonia-oxidizing archaeon from the open ocean. *Proc. Natl. Acad. Sci. U.S.A.* 112, 1173–1178. doi: 10.1073/pnas.1416223112
- Sarmiento, J. L., Herbert, T. D., and Toggweiler, J. R. (1988). Mediterranean nutrient balance and episodes of anoxia. *Global Biogeochem. Cycles* 2, 427–444. doi: 10.1029/GB002i004p00427
- Schleper, C., Jurgens, G., and Jonuscheit, M. (2005). Genomic studies of uncultivated archaea. *Nat. Rev. Microbiol.* 3, 479–488. doi: 10.1038/nrmicro1159
- Sintes, E., Bergauer, K., De Corte, D., Yokokawa, T., and Herndl, G. J. (2013). Archaeal *amoA* gene diversity points to distinct biogeography of ammonia-oxidizing Crenarchaeota in the ocean. *Environ. Microbiol.* 15, 1647–1658. doi: 10.1111/j.1462-2920.2012.02801.x
- Sintes, E., De Corte, D., Haberleitner, E., and Herndl, G. J. (2016). Geographic distribution of archaeal ammonia oxidizing ecotypes in the Atlantic Ocean. *Front. Microbiol.* 7:77. doi: 10.3389/fmicb.2016.00077
- Sintes, E., De Corte, D., Ouilion, N., and Herndl, G. J. (2015). Macroecological patterns of archaeal ammonia oxidizers in the Atlantic Ocean. *Mol. Ecol.* 24, 4931–4942. doi: 10.1111/mec.13365

- Siokou-Frangou, I., Christaki, U., Mazzocchi, M. G., Montresor, M., Ribera d'Alcalá, M., Vagué, D., et al. (2010). Plankton in the open Mediterranean Sea: a review. *Biogeoscience* 7, 1543–1586. doi: 10.5194/bg-7-1543-2010
- Smedile, F., Messina, E., La Cono, V., Tsoy, O., Monticelli, L. S., Borghini, M., et al. (2013). Metagenomic analysis of hadopelagic microbial assemblages thriving at the deepest part of Mediterranean Sea, Matapan-Vavilov Deep. *Environ. Microbiol.* 15, 167–182. doi: 10.1111/j.1462-2920.2012.02827.x
- Smith, D. C., and Azam, F. (1992). A simple, economical method for measuring bacterial protein synthesis rates in seawater using <sup>3</sup>H-leucine. *Mar. Microb. Food Webs* 6:107.
- Steinberg, D. K., Van Mooy, B. A., Buesseler, K. O., Boyd, P. W., Kobari, T., and Karl, D. M. (2008). Bacterial vs. zooplankton control of sinking particle flux in the ocean's twilight zone. *Limnol. Oceanogr.* 53, 1327–1338. doi: 10.4319/lo.2008.53.4.1327
- Stieglmeier, M., Klingl, A., Alves, R. J., Rittmann, S. K., Melcher, M., Leisch, N., et al. (2014). *Nitrososphaera viennensis* gen. nov., sp. nov., an aerobic and mesophilic, ammonia-oxidizing archaeon from soil and a member of the archaeal phylum Thaumarchaeota. *Int. J. Syst. Evol. Microbiol.* 64, 2738–2752. doi: 10.1099/ijls.0.063172-0
- Strickland, J. D. H., and Parsons, T. R. (1972). A practical handbook of sea water analysis *Bull. Fish. Res. Board Can.* 169, 1–311.
- Swan, B. K., Martinez-Garcia, M., Preston, C. M., Sczyrba, A., Woyke, T., Lamy, D., et al. (2011). Potential for chemolithoautotrophy among ubiquitous bacteria lineages in the dark ocean. *Science* 333, 1296–1300. doi: 10.1126/science.1203690
- Takahashi, T., Broecker, W. S., and Langer, S. (1985). Redfield ratio based on chemical data from isopycnal surfaces. *J. Geophys. Res.* 90, 6907–6924. doi: 10.1029/JC090iC04p06907
- Tamburini, C., Boutrif, M., Garel, M., Colwell, R. R., and Deming, J. W. (2013). Prokaryotic responses to hydrostatic pressure in the ocean—a review. *Environm. Microbiol.* 15, 1262–1274. doi: 10.1111/1462-2920.12084
- Tamburini, C., Garcin, J., and Bianchi, A. (2003). Role of deep-sea bacteria in organic matter mineralization and adaptation to hydrostatic pressure conditions in the NW Mediterranean Sea. *Aquat. Microb. Ecol.* 32, 209–218. doi: 10.3354/ame032209
- Tamburini, C., Garel, M., Al Ali, B., Merigot, B., Kriwi, P., Charriere, B., et al. (2009). Distribution and activity of Bacteria and Archaea in the different water masses of the Tyrrhenian Sea. *Deep-Sea Res. Part II* 56, 700–712. doi: 10.1016/j.dsr2.2008.07.021
- Tamura, K., Peterson, D., Peterson, N., Stecher, G., Nei, M., and Kumar, S. (2011). MEGA5: molecular evolutionary genetics analysis using maximum likelihood, evolutionary distance, and maximum parsimony methods. *Mol. Biol. Evol.* 28, 2731–2739. doi: 10.1093/molbev/msr121
- Thingstad, T. F., Krom, M. D., Mantoura, R. F. C., Flaten, G. F., Groom, S., Herut, B., et al. (2005). Nature of phosphorus limitation in the ultra-oligotrophic Central-Eastern Mediterranean. *Science* 309, 1068–1071. doi: 10.1126/science.1112632
- Tolar, B. B., Ross, M. J., Wallsgrove, N. J., Liu, Q., Aluwihare, L. I., Popp, B. N., et al. (2016). Contribution of ammonia oxidation to chemoautotrophy in Antarctic coastal waters. *ISME J.* 10, 2605–2619. doi: 10.1038/ismej.2016.61
- Van Wambeke, F., Christaki, U., Bianchi, M., Psara, S., and Tselepidis, A. (2000). Heterotrophic bacterial production in the Cretan Sea (NE Mediterranean). *Prog. Oceanogr.* 46, 205–216. doi: 10.1016/S0079-6611(00)00019-7
- Varela, M. M., van Aken, H. M., Sintes, E., and Herndl, G. J. (2008). Latitudinal trends of Crenarchaeota and Bacteria in the meso- and bathypelagic water masses of the Eastern North Atlantic. *Environ. Microbiol.* 10, 110–124. doi: 10.1111/j.1462-2920.2007.01437.x
- Varela, M. M., van Aken, H. M., Sintes, E., Reinthaler, T., and Herndl, G. J. (2011). Contribution of Crenarchaeota and Bacteria to autotrophy in the North Atlantic interior. *Environ. Microbiol.* 13, 1524–1533. doi: 10.1111/j.1462-2920.2011.02457.x
- Weber, C. F., and King, G. M. (2007). Physiological, ecological, and phylogenetic characterization of *Stappia*, a marine CO<sub>2</sub>-oxidizing bacterial genus. *Appl. Environ. Microbiol.* 73, 1266–1276. doi: 10.1128/AEM.01724-06
- Widdel, F., and Bak, F. (1992). “Gram-negative mesophilic sulfate-reducing bacteria,” in *The Prokaryotes*, eds A. Balows, H. G. Trüper, M. Dworkin, W. Harder and K.-H. Schleifer (New York, NY: Springer), 3352–3378.
- Williams, P. J., Quay, P. D., Westberry, T. K., and Behrenfeld, M. J. (2013). The oligotrophic ocean is autotrophic. *Annu. Rev. Mar. Sci.* 5, 535–549. doi: 10.1146/annurev-marine-121211-172335
- Wu, Y. H., Jian, S. L., Meng, F. X., Tohty, D., Wang, C. S., and Xu, X. W. (2016). *Kordiimonas lipolytica* sp. nov., isolated from seawater. *Int. J. Syst. Evol. Microbiol.* 66, 2198–2204. doi: 10.1099/ijsem.0.001007
- Wuchter, C., Abbas, B., Coolen, M. J., Herfort, L., van Bleijswijk, J., Timmers, P., et al. (2006). Archaeal nitrification in the ocean. *Proc. Natl. Acad. Sci. U.S.A.* 103, 12317–12322. doi: 10.1073/pnas.0600756103
- Yakimov, M. M., La Cono, V., Denaro, R., D'Auria, G., Decembrini, F., Timmis, K. N., et al. (2007). Primary producing prokaryotic communities of brine, interface and seawater above the halocline of deep anoxic lake L'Atalante, Eastern Mediterranean Sea. *ISME J.* 1, 743–755. doi: 10.1038/ismej.2007.83
- Yakimov, M. M., La Cono, V., Spada, G. L., Bortoluzzi, G., Messina, E., Smedile, F., et al. (2015). Microbial community of the deep-sea brine Lake Kryos seawater–brine interface is active below the chaotricity limit of life as revealed by recovery of mRNA. *Environ. Microbiol.* 17, 364–382. doi: 10.1111/1462-2920.12587
- Yakimov, M. M., La Cono, V., Slepak, V. Z., La Spada, G., Arcadi, E., Messina, E., et al. (2013). Microbial life in the Lake Medee, the largest deep-sea salt-saturated formation. *Sci. Rep.* 3:3554. doi: 10.1038/srep03554
- Yakimov, M. M., La Cono, V., Smedile, F., Crisafi, F., Arcadi, E., Leonardi, M., et al. (2014). Heterotrophic bicarbonate assimilation is the main process of de novo organic carbon synthesis in hadal zone of the Hellenic Trench, the deepest part of Mediterranean Sea. *Environ. Microbiol. Rep.* 6, 709–722. doi: 10.1111/1758-2229.12192
- Yakimov, M. M., Cono, V. L., Smedile, F., DeLuca, T. H., Juárez, S., Ciordia, S., et al. (2011). Contribution of crenarchaeal autotrophic ammonia oxidizers to the dark primary production in Tyrrhenian deep waters (Central Mediterranean Sea). *ISME J.* 5, 945–961. doi: 10.1038/ismej.2010.197
- Zacccone, R., Boldrin, A., Caruso, G., La Ferla, R., Maimone, G., Santinelli, C., et al. (2012). Enzymatic activities and prokaryotic abundance in relation to organic matter along a West-East Mediterranean transect (TRANSMED cruise). *Microb. Ecol.* 63, 54–66. doi: 10.1007/s00248-012-0011-4
- Zacccone, R., Caruso, G., Azzaro, M., Azzaro, F., Crisafi, E., Decembrini, F., et al. (2010). Prokaryotic activities and abundance in pelagic areas of the Ionian Sea. *Chem. Ecol.* 26, 169–197. doi: 10.1080/02757541003772914
- Zheng, H. Y., Liu, Y., Gao, X. Y., Ai, G. M., Miao, L. L., and Liu, Z. P. (2012). Characterization of a marine origin aerobic nitrifying–denitrifying bacterium. *J. Biosci. Bioeng.* 114, 33–37. doi: 10.1016/j.jbiosc.2012.02.025

**Conflict of Interest Statement:** The authors declare that the research was conducted in the absence of any commercial or financial relationships that could be construed as a potential conflict of interest.

Copyright © 2018 La Cono, Ruggeri, Azzaro, Crisafi, Decembrini, Denaro, La Spada, Maimone, Monticelli, Smedile, Giuliano and Yakimov. This is an open-access article distributed under the terms of the Creative Commons Attribution License (CC BY). The use, distribution or reproduction in other forums is permitted, provided the original author(s) or licensor are credited and that the original publication in this journal is cited, in accordance with accepted academic practice. No use, distribution or reproduction is permitted which does not comply with these terms.